Mitochondrial STAT3 regulates proliferation of tissue stem cells.

Margherita Peron[1*], Giacomo Meneghetti[1*], Alberto Dinarello[1*], Laura Martorano[1], Riccardo M. Betto[2], Nicola Facchinello[1], Natascia Tiso[1], Graziano Martello[2^], Francesco Argenton[1^].

[1] Department of Biology, University of Padova, Padova, Italy,

[2] Department of Molecular Medicine, University of Padova, Padova, Italy.

* The authors contributed equally to this work.

^ Co-corresponding authors

ABSTRACT

The STAT3 transcription factor, acting both in the nucleus and mitochondria, is needed to maintain embryonic stem cell pluripotency and promote proliferation. In this work, using zebrafish, we determined *in vivo* that mitochondrial STAT3 regulates mtDNA transcription in embryonic and larval stem cell niches and that this activity is fundamental in determining proliferation rates. To dissect the molecular requirements for mitoSTAT3 functions, we used drugs and missense mutations to kinase-targeted STAT3 residues. As a result, we demonstrated that STAT3 import inside mitochondria requires Y705 phosphorylation by Jak2, while its mitochondrial transcriptional activity, as well as its replication potential, depends on the MAPK target S727. Moreover, while STAT3-dependent mtDNA transcription is needed and sufficient to induce cell proliferation, it is not required to maintain stem-like phenotype in the tectal niche. Surprisingly, STAT3-dependent increase of mitochondrial transcription seems independent from STAT3 binding to DNA and does not originate from STAT3 regulation of mtDNA replication.

INTRODUCTION

The investigation of the role of Signal Transducer and Activator of Transcription 3 (STAT3) pathway in human diseases represents, to date, one of the most exciting developments in modern medicine (O'Shea *et al.*, 2015). Many of the major human malignancies display elevated levels of constitutively activated STAT3 (Johnston and Grandis, 2011). Most interestingly, recent data report that STAT3 target genes are overexpressed in tumour-initiating cancer stem cells (Fouse and Costello, 2013; Wei *et al.*, 2014; Ghoshal *et al.*, 2016). Notably, being the key mediator of Leukemia Inhibitory Factor (LIF)-dependent

1

Embryonic Stem Cells (ESC) self-renewal *in vitro* (Burdon *et al*., 1999; Matsuda *et al*., 1999), STAT3 promotes the maintenance and induction of ESC naïve pluripotency (Martello *et al.*, 2013).

STAT3 transcriptional activity is regulated by phosphorylation of two separate residues. When Janus kinase 2 (JAK2) phosphorylates its tyrosine 705 (Y705), STAT3 can dimerize, enter the nucleus, and trigger transcription of its target genes (Ni *et al.*, 2004). On the other hand, the function of serine 727 (S727) phosphorylation remains controversial; pS727 has been reported to have both down- and up-regulatory effects on STAT3 transcriptional activity (Quin *et al.*, 2008; Shi *et al.*, 2006). More recently, it has been demonstrated that pY705 is absolutely required for STAT3-mediated mESC self-renewal, while pS727 is dispensable, serving only to promote proliferation and optimal pluripotency (Huang *et al.*, 2014). Notably, zebrafish mutants lacking maternal and zygotic Stat3 expression display transient axis elongation defects due to reduced cell proliferation during embryogenesis (Liu *et al*., 2017). Additionally, it has been demonstrated that in zebrafish Stat3 is transcriptionally active in stem cells of highly proliferative tissues like tectum opticum, hematopoietic tissue and intestine (Peron *et al*., 2020).

Besides its canonical nuclear function, a pool of STAT3 has been reported also in the mitochondrion of different cell types, thus including this transcription factor in the large family of dual-targeted proteins with a nuclear and mitochondrial life (Wegrzyn *et al.*, 2009; Mantel *et al.*, 2012). A recently discovered subcellular localization of Stat3 is the Endoplasmatic Reticolum (ER), where it controls the release of Ca^{2+}, with consequences on the mitochondrial Ca^{2+} levels and on the life-death cell decision. This function is crucial for the maintenance in the tumour niche of apoptosis-resistant cells (Avalle *et al*.,2019). Although the mechanisms of action of mitoSTAT3 are still debated, approximately one-tenth of cytosolic STAT3 has been shown to be in the mitochondria, (Szczepanek *et al.*, 2011). Several mitochondrial roles for STAT3 have been proposed so far, such as the interaction with OXPHOS complexes I and II, the direct binding to the d-loop regulatory region of mitochondrial DNA (mtDNA), the regulation of mitochondrial permeability transition pore (Wegrzyn *et al.,* 2009; Macias *et al.*, 2014; Meier and Larner, 2014). Carbognin and colleagues (2016) have recently showed *in vitro* that STAT3 is able to trigger mitochondrial gene expression and cell proliferation, thus suggesting a possible connection between this most prominent effect on ESC and a "non-canonical mitochondrial STAT3 (mitoSTAT3) pathway". On the other hand, a clear function of mitoSTAT3 and the mechanism leading to its activation and translocation are to date not well-understood. Previous *in vitro* studies

2

suggested that the S727 phosphorylation by ERK (MAPK) kinases may be required for STAT3 mitochondrial activity (Gough *et al.*, 2013) and it seems necessary to restore complexes I and II activities in *Stat3*^{-/-} cells (Wegrzin *et al.*, 2009). Moreover, p727 STAT3 targeted to the mitochondria is described to promote Ras-dependent transformation in human bladder carcinoma cells (Gough *et al.*, 2009). Notably, the role of other post-translational modifications on mitoSTAT3 activity have not been investigated yet. Zebrafish is a widely used organism for expression and functional analysis of proteins due to its transparent body and external fertilization. Knowing that Stat3 protein and all its functional domains are highly conserved in zebrafish (Liang *et al.*, 2012, Oates *et al.,* 1999) we used this animal model to study the non-canonical Stat3 pathway *in vivo*. In this paper we demonstrate the dependence of mitoSTAT3 activities from both Y705 and S727 phosphorylations, hence, that mitoSTAT3 mitochondrial function relies on both ERK and JAK2 kinases activation. On the other hand, our data show that mitoSTAT3 modulates mitochondrial transcription without binding to canonical STAT3 Binding Elements (SBE), consistently with the huge differences between the eucariotic and the procariotic transcriptional machineries operating in the nucleus and mitochondria, respectively. Moreover, we directly linked the STAT3-dependent regulation of tissue stem cells proliferation to mitochondrial transcriptional activity of zebrafish embryos, thus supporting the idea of a role in cancer development for the "non-canonical", mitoSTAT3 pathway.

RESULTS

mitoSTAT3 regulates cell proliferation in the PML of the TeO through mtDNA transcription

According to recent publications, a portion of STAT3 localizes to mitochondria, where it is supposed to bind to mtDNA and act as a mitochondrial transcription factor able to induce cell proliferation in ESC (Macias *et al.*, 2014; Carbognin *et al.*, 2016). It can be easily assessed that mtDNA-encoded genes, as well as the cellular proliferation marker *pcna*, are, by default, particularly expressed in regions also labelled by *stat3* transcripts, such as the inner retina and the Peripheral Midbrain Layer (PML) of the Tectum Opticum (TeO) (Fig. 1; Fig. 2A), which serves as progenitor source for tectal and torus neurons in the embryo (Galant *et al.*, 2016). Due to the polycistronic nature of mtDNA-encoded genes, that results in stoichiometric mtDNA transcription (Taanman, 1999), we decided to use the mitochondrial gene *mt_nd2* as a hallmark of global mitochondrial gene expression, since its expression

3

profile is already described in zebrafish (Thisse *et al.*, 2001). To understand whether Stat3 mitochondrial activity regulates mtDNA transcription and promotes proliferation also *in vivo*, we injected zebrafish fertilized eggs with mRNA of a mitochondria-targeted murine form of *Stat3* provided with a nuclear export domain that makes it unable to localize in the nucleus (*MLS_mStat3_NES*) (Fig. S1 A). This artificial protein a) efficiently localizes only inside the mitochondrion in transfected mESC, as revealed by its co-expression with the mitochondrial marker ATAD3 on ES cells (Fig. S1 C) as well as in Zebrafish (Fig. S6 A,B),; b) is completely devoid of nuclear functions as assessed by qRT-PCR analysis of the most direct *Stat3* target gene, *Socs3* (Fig. S1 B).

Thus, when *MLS_mStat3_NES* mRNA was introduced into zebrafish embryos we could observe, both by *in situ* hybridization and qRT-PCR, a significant increase of mitochondrial transcription, that reached a peak at 48 hpf (Fig. 2A-A', C). It is worth noting that, as assayed by *pcna* analysis, overexpression of *MLS_mStat3_NES* mRNA also induced a proportional increase of proliferating cells in the same tissues where mitochondrial transcription was stimulated, i.e. the PML (Fig. 2 B-B', C, D). On the other hand, we did not find any difference in mtDNA content when comparing injected and control embryos, meaning that the effect of mitoSTAT3 on mitochondrial transcription is not due to increased mtDNA replication or mitochondrial biogenesis (Fig. 2E).
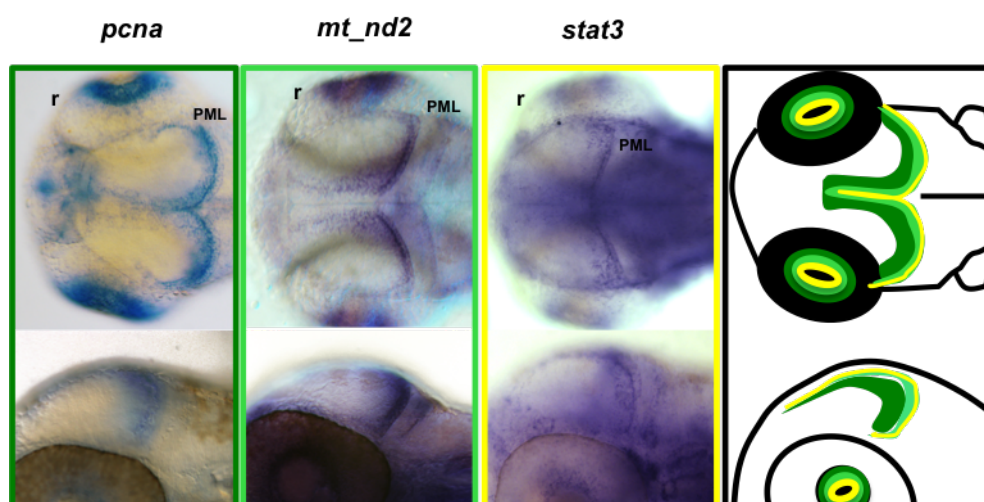

Fig. 1 *Stat3* **mRNA is co-expressed with proliferation and mtDNA transcription markers in the TeO of zebrafish embryos.** WISH on 48-hpf zebrafish WT embryos using *stat3, pcna* and *mt_nd2* antisense mRNA probe shows co-expression of the three transcripts in the PML region of the TeO; r=retina; PML= Peripheral Midbrain Layer.

Importantly, chemical inhibition of mitochondrial transcription by using Balapiravir (Feng *et al.*, 2015) was able to abolish *MLS_Stat3_NES* effects on proliferation (Fig 2 A'', B'', D), thus

4

providing some evidence, *in vivo,* that replication of highly proliferating PML cells in the developing TeO of zebrafish embryos depends on mitoSTAT3-driven expression of mitochondrial genes.

Since putative STAT3 binding elements (SBE) have been identified in the mitochondrial D-Loop (the mitochondrial transcriptional initiation site) (Macias *et al.*, 2014) and STAT3 was found to immunoprecipitate together with the mitochondrial D-Loop in mouse ES cells (Carbognin *et al.,* 2016), we wondered whether mitoSTAT3 can regulate gene expression in mitochondrion by interacting with these putative mitochondrial SBE. Surprisingly, a form of mitochondrial STAT3 mutated in the DNA binding domain (STAT3 458-466 VVV-AAA) (MLS_mStat3_ΔDNAbd_NES), thus unable to bind SBE (Horvath *et al.*, 1995), retained its ability to activate *mt_nd2* transcription at comparable levels with respect to wild type (WT) mitoSTAT3 on zebrafish embryos (Fig. 2F; Fig. S2 A). However, as evidenced on mouse ESC, this form mutated on its DNA binding domain, is still able to co-localize with ATAD3, a mitochondrial nucleoids marker, (Fig. 2G, Fig. S5). This result suggests that, unlike nuclear STAT3, mitoSTAT3 does not regulate mtDNA transcription by direct binding to canonical STAT3 cis-responsive elements, even though it is recruited in proximity of mtDNA.

Finally, to assess the effect of mitochondrial STAT3 on neural progenitor number during zebrafish embryogenesis, we observed the expression levels of *sox9b*, *her4.1* and *her5* neural precursor's markers. Sox9b transcription factor, the functional orthologous of mammalian SOX9 (Kluever et al., 2005), is known to induce and maintain different types of stem cells including mammalian neural stem cells in the Central Nervous System (CNS) (Scott *et al.*, 2010; Martini *et al.*, 2013; Jo *et al.*, 2014).
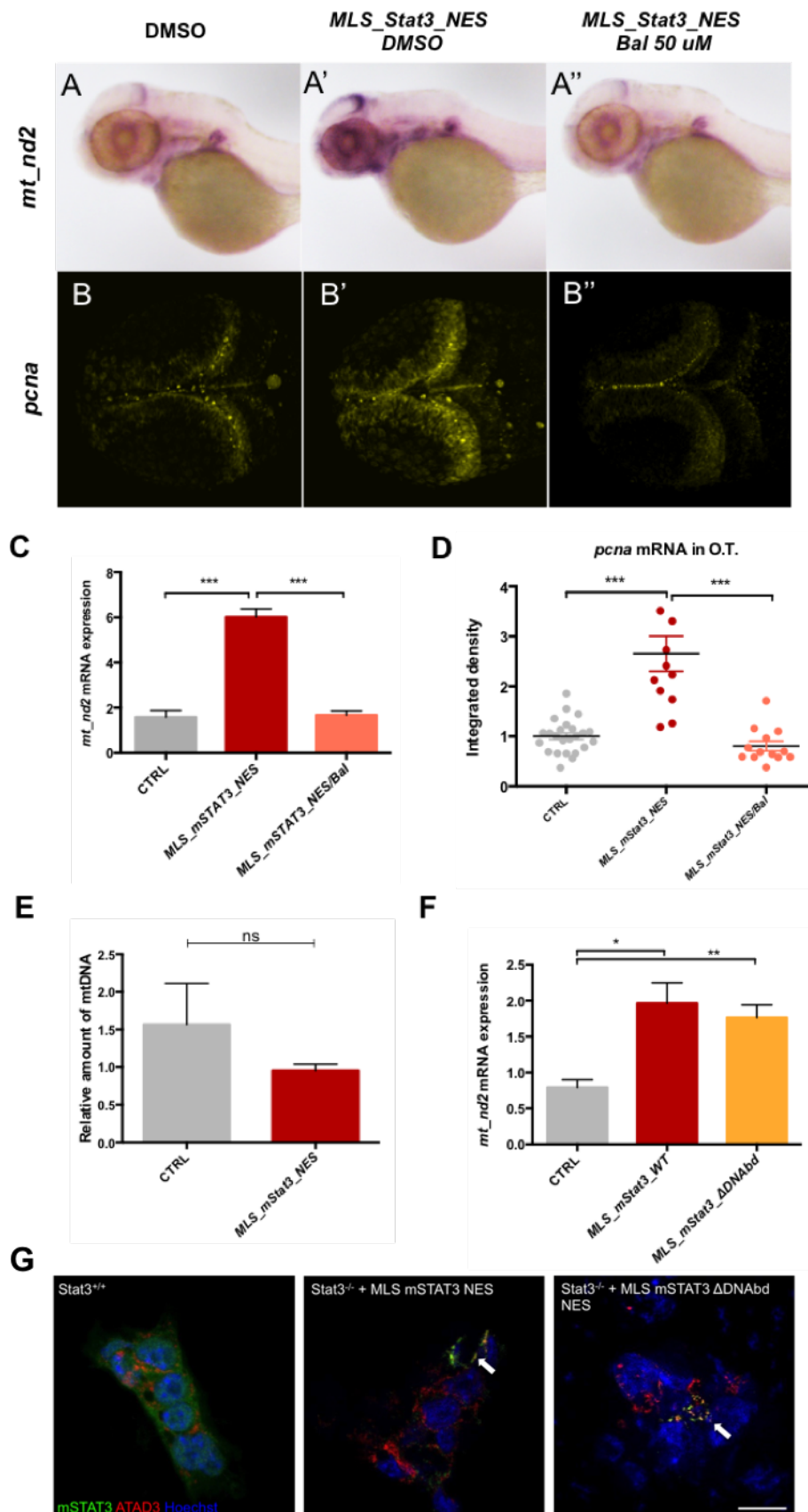
Fig. 2 **mitoSTAT3 regulates proliferation through mitochondrial DNA transcription.** A-A": WISH with anti-*mt_nd2* mRNA probe representing mitochondrial gene transcription in uninjected embryos (A), embryos injected with *MLS_mStat3_NES* mRNA (A'), and injected embryos treated with 50 µM Balapiravir (A"). B-B": FISH with *pcna* probe in the TeO of

6

uninjected embryos (B), embryos injected with *MLS_mStat3_NES* mRNA (B'), and injected embryos treated with 50 µM Balapiravir (B"). C: qRT-PCR showing *mt_nd2* gene expression after injection of *MLS_mStat3_NES* mRNA and treatment with Balapiravir at 48 hpi; *zgapdh* was used as internal control (p-values= 0,0007;0,0005). D: Fluorescence quantification of *pcna* mRNA expression in the TeO (n=12) (p-values= <0,0001;0,0108,0,0122). E: Relative amount of mtDNA in embryos injected with *MLS_mStat3_NES* mRNA and uninjected controls at 48 hpf. Mean dCt values were calculated as Ct of *mt_nd1* (mitochondrial encoded gene) minus Ct of *polg1* (nuclear encoded gene) (p-value= 0,3295). F: qRT-PCR showing *mt_nd2* gene expression after injection of *MLS_mStat3_NES* or *MLS_mStat3_ΔDNAbd_NES* mRNA in 48-hpf embryos; *zgapdh* was used as internal control (p-values= 0,0184; 0,0093). G: immunofluorescence on ES cells transfected with the constructs used on zebrafish experiments and stained with anti-STAT3 (green) and anti-ATAD3 (red) Ab and DAPI.
Statistical analysis in C-F was performed by unpaired t-test on 3 independent biological samples (where n not specified)*.* ns: not significant; *p<0,05; **p<0.01; ***p<0.001; error bars=SEM.

Furthermore, *her4.1* (orthologous to mammalian *Hes5*) and *her5* (orthologous to mammalian *Hes7*) transcripts, were recently demonstrated to respectively mark neuroepithelial and radial glial precursor cells in the TeO, the two populations of neural precursors in zebrafish (Galant *et al.*, 2016). Interestingly, no significant difference in the expression of any of the three embryonic undifferentiated neural markers was detectable in the TeO of 48-hpf embryos injected with *MLS_Stat3_NES* with respect to uninjected controls (Fig. 3)*.* This finding leads to the conclusion that mitochondrial STAT3 has a role in regulating proliferation of neural cells in the Tectal Proliferation Zone (TPZ) of the TeO but not in maintaining the undifferentiated state of these neural precursors.
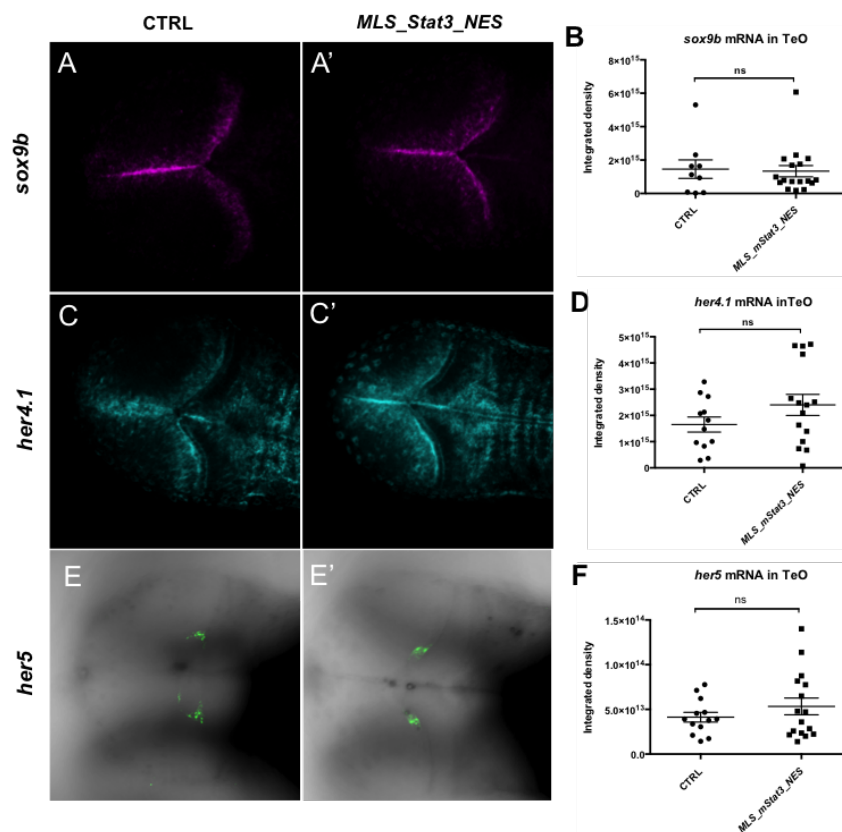
Fig. 3 mitoSTAT3 is not affecting stemness marker expression in the PML of the TeO.
A,A': FISH with anti-*sox9b* probe in the TeO of embryos injected with *MLS_mStat3_NES* mRNA and uninjected controls at 48 hpf. B: Fluorescence quantification of *sox9b* mRNA expression in the TeO (n=10) (p-value= 0,8438). C,C': FISH with anti-*her4* probe in the TeO of embryos injected with *MLS_mStat3_NES* mRNA and uninjected controls at 48 hpf. D: Fluorescence quantification of *her4* mRNA expression in the TeO (n=12) (p-value= 0,1615). E,E': FISH with anti-*her5* probe in the TeO of embryos injected with *MLS_mStat3_NES* mRNA and uninjected controls at 48 hpf. F: Fluorescence quantification of *her5* mRNA expression in the TeO (n=12) (p-value= 0,3073). Statistical analysis was performed by unpaired t-test on indicated number of samples. ns: not significant; error bars=SEM.

Mitochondrial STAT3 transcriptional activity relies on both S727 and Y705 phosphorylations

STAT3 nuclear activity is known to be controlled by JAK2-mediated phosphorylation of Y705 residue, which also ensures STAT3 monomers stability in the cytoplasm (Becker *et al.,* 1998). On the other hand, phosphorylation on STAT3 S727 by the MAPK/ERK pathway (Ras-Raf-MEK-ERK pathway) is known, from *in vitro* studies, to enhance the Electron Transport Chain (ETC) (Wegrzyn *et al.*, 2009) as well as to promote cell proliferation and optimal pluripotency (Huang *et al.*, 2014). To verify *in vivo* the post-translational requirements, and to test whether also mitoSTAT3 activity requires Y705 phosphorylation, we decided to inject 1-cell stage zebrafish embryos with mRNAs encoding variants of murine *Stat3*. In particular, we compared the activity of WT STAT3 (without the MLS) with two

mutated forms, Y705F and S727A, able to prevent phosphorylation of residues 705 and 727, respectively. Interestingly, when embryos were injected with the WT isoform, quantitative analysis of fluorescent *in situ* hybridization revealed a significant increase of mitochondrial transcription in the PML of the TeO (Fig. 4 A,B), even though qRT-PCR analysis on homogenized embryos did not result in any significant variation of global *mt_nd2* gene expression (Fig.4 C,D). Notably, when injecting either Y705F or S727A isoforms of a STAT3 not provided with a constitutive mitochondrial import signal, no significant stimulation of mitochondrial transcription in the PML population was detected, either using *in situ* hybridization or qRT-PCR (Fig. 4 A-D; Fig. S2 B). In conclusion, both phosphorylations are needed for STAT3-mediated increase of mtDNA transcription in the PML. On the other hand, when the mutated isoforms are forcedly targeted only to the mitochondrion (by using both the MLS and the NES), the S727A mutation prevented mitoSTAT3-mediated activation of *mt_nd2* gene expression, while the STAT3-Y705F mutated isoform retained its mitochondrial transcriptional activity (Fig. 4 E,F; Fig. S2 C). This implies that Y705 is essential for precise transport of STAT3 from the cytoplasm to mitochondria.
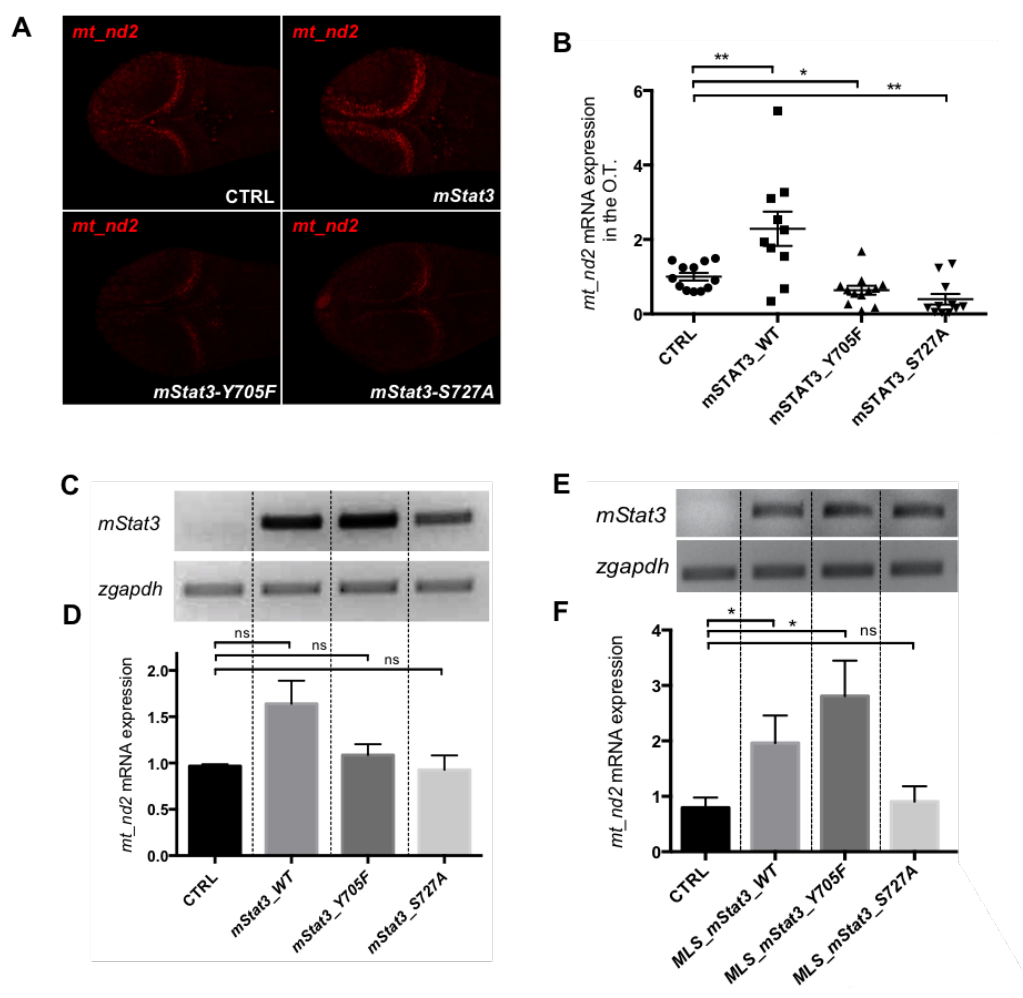
Fig. 4 **mitoSTAT3 transcriptional activity relies on both S727 and Y705 phosphorylations.** A: FISH with *mt_nd2* probe in the TeO of 48 hpf embryos injected with mRNA encoding the indicated isoforms of *mStat3*. B: Fluorescence quantification of *mt_nd2* mRNA expression in the TeO (n=10) (p-values= 0,0074; 0,0307; 0,0023). C: qRT-PCR analysis of *mStat3* transcripts detected at 48 hpf/hpi in embryos injected with indicated form of *mStat3* mRNA; *zgapdh* was used as internal control. D: qRT-PCR analysis of *mt_nd2* transcript levels at 48 hpf/hpi normalized to *zgapdh* (p-values= 0,0888; 0,1899; 0,8334). E: qRT-PCR analysis of MLS_*mStat3* transcripts detected at 48 hpf/hpi in embryos injected with indicated form of mitochondria-targeted *mStat3* mRNA; *zgapdh* was used as internal control. D: qRT-PCR analysis of *mt_nd2* transcript levels at 48 hpf/hpi normalized to *zgapdh* (p-values= 0,0184; 0,0355; 0,5846). Statistical analysis was performed by unpaired t-test on 3 independent biological samples (where n not specified). ns: not significant; *p<0,05; **p<0.01; error bars=SEM.

To further elucidate the localization of different mutated forms of STAT3, we performed immunofluorescence analysis on mouse *stat3*^{-/-} ESC transiently transfected with different forms of STAT3. Transient expression of STAT3 Y705F was not enough informative and immunofluorescence was not clear. For this reason we decided to test different approaches to better understand the correct localization of this mutated form of STAT3. As reported in Fig. 5 C, isolation of mitochondria was performed and protein extracts were used for western

10

blot analysis: surprisingly, STAT3 Y705F seemed to precipitate together with mitochondria. Hence, we hypothesised that the mutation at the level of the tyrosine 705 prevents the correct migration of the protein through the outer mitochondrial membrane (OMM). To test this hypothesis, we decided to perform DAB (3,3'-Diaminobenzidine) immunohistochemistry on ESC expressing STAT3 Y705F protein. As shown in Fig. 5 D, WT STAT3 localises both in nuclei and mitochondria, and MLS_STAT3_NES is visible only in mitochondria, however, STAT3 Y705F forms clots in the cytoplasm which surround organelles, but it does not pass through the OMM. These results confirm that Y705 is essential for the correct import of STAT3 inside the mitochondrion.
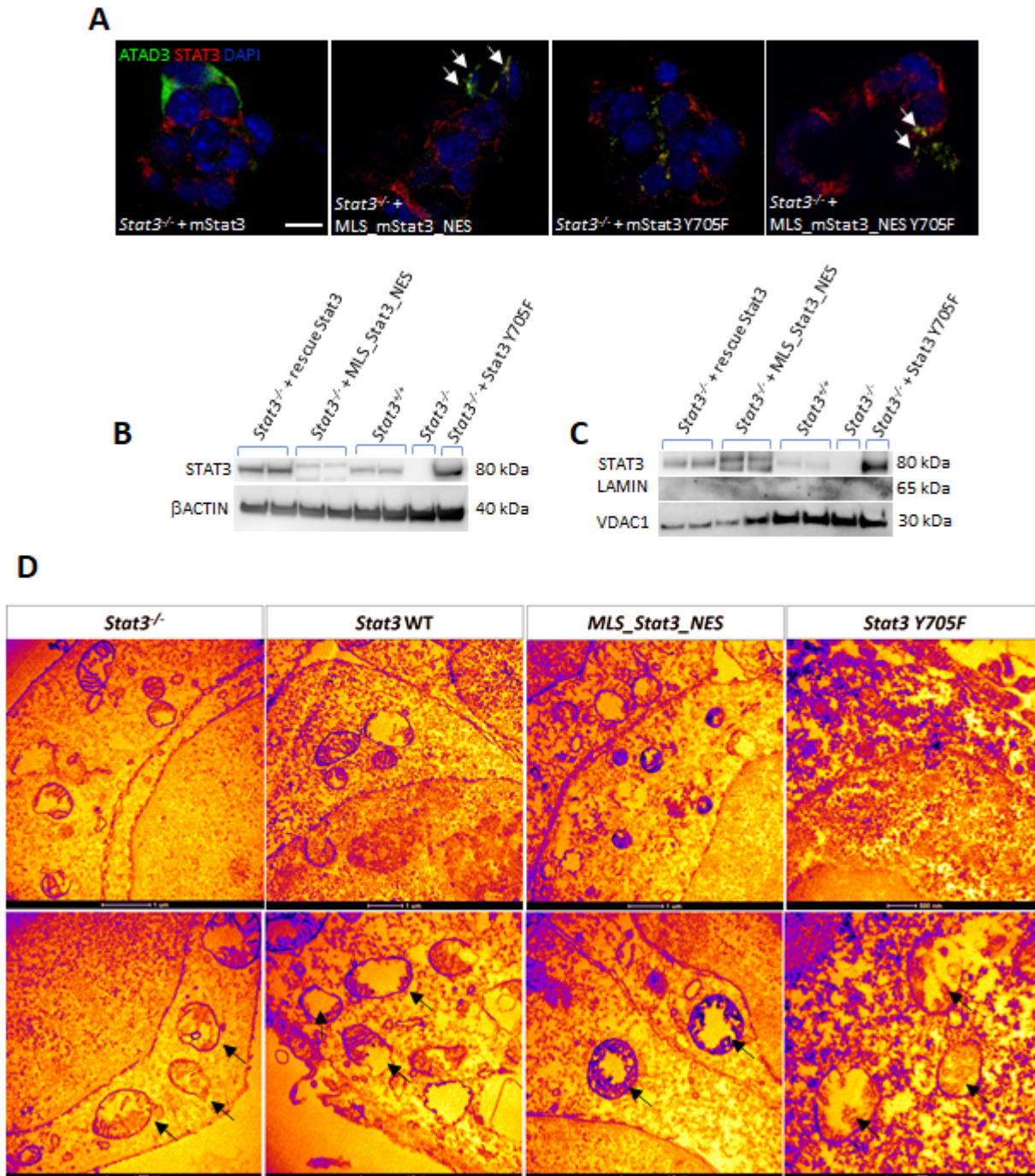
Fig. 5 **Y705 phosphorylation is necessary for the correct localization of STAT3 in the mitochondrion.** A: immunofluorescence with anti-STAT3 and anti-ATAD3 Ab on ES cells transfected with the constructs used on zebrafish experiments. Arrows indicate the colocalization of ATAD and STAT3. B: western blot of total STAT3 in ESCs extracts, β-actin was used as a loading control. C: western blot of mitochondrial STAT3 from ESCs mitochondrial extracts, VDAC1 was used as a mitochondrial loading control, Lamin was used as a nuclear loading control. D: representative pictures of DAB immunohistochemistry on ESCs acquired with TEM and pseudo-colored to enhance contrast: positive is in purple and negative in yellow.. Arrows indicate mitochondria.

STAT3 S727 phosphorylation is needed for mitoSTAT3-driven promotion of cell proliferation in the TPZ

As phosphorylation to STAT3 S727 seems necessary for mitoSTAT3-driven mtDNA transcription, we tested whether this post-transcriptional modification is also required for the increase of TPZ proliferation downstream of mitochondrial RNA production in the TPZ.
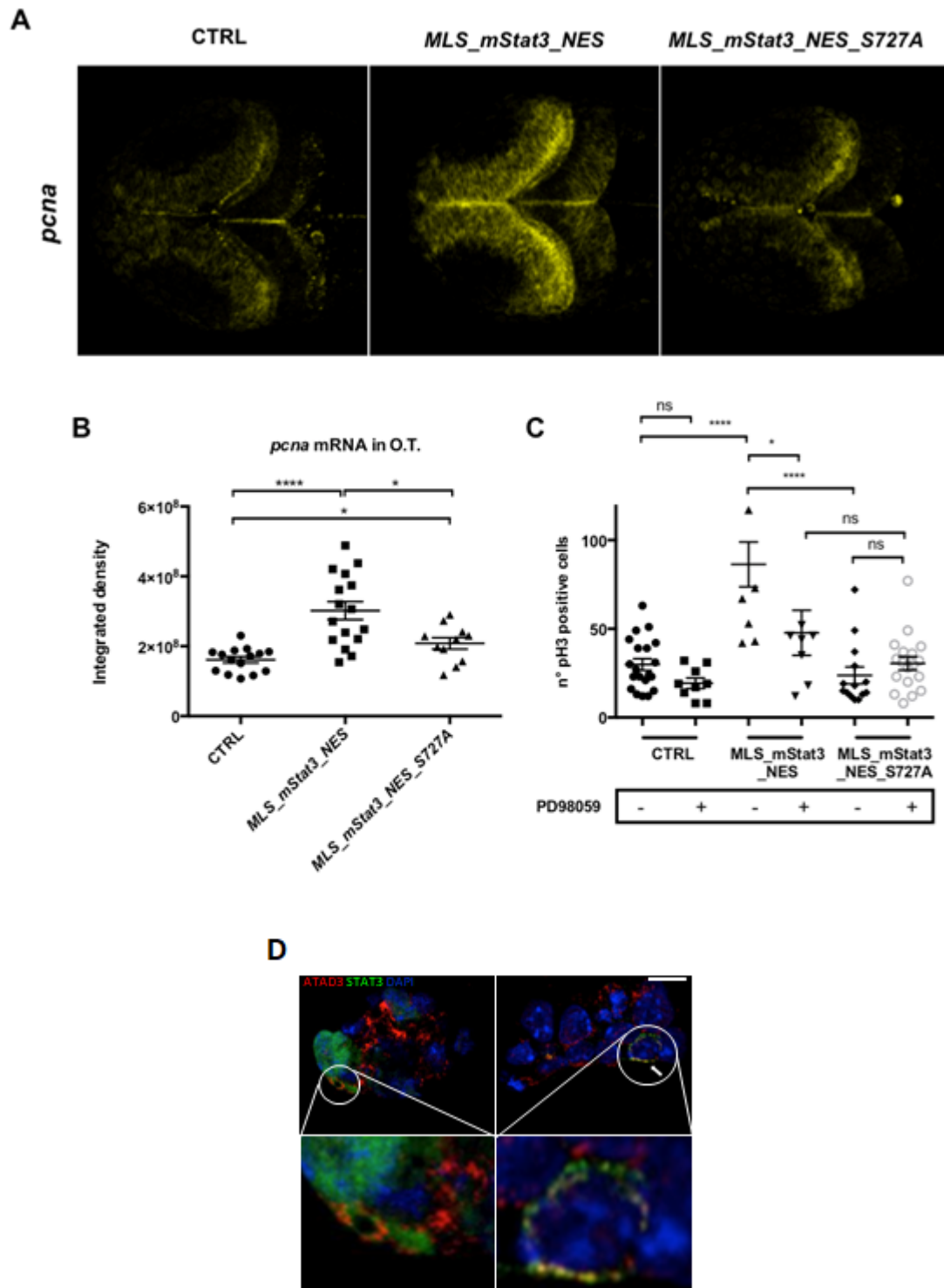

Fig. 6 **mitoSTAT3-dependent activation of cell proliferation in the TeO depends on S727 phosphorylation.** A: FISH with anti-*pcna* probe in the TeO of 48 hpf embryos injected

13

with *MLS_mStat3_NES* and *MLS_mStat3_S727A_NES* mRNA. B: Fluorescence quantification of *pcna* mRNA expression in the TeO (n=12) (p-values= <0,0001; 0,0108; 0,0122). C: number of pH3 positive cells in the head of 48 hpf embryos after injection with indicated forms of mitochondria-targeted Stat3 and treatment with either 12,5 uM PD98059 or DMSO (p-value= 0,0562; <0,0001; 0,0483; <0,0001; 0,0974; 0,2721). Statistical analysis was performed by unpaired t-test on 3 independent biological samples (where n not specified). *p<0,05; ****p<0.0001; error bars=SEM. D: immunofluorescence with anti-STAT3 and anti-ATAD3 Ab on ES cells transfected with the constructs used on zebrafish experiments. Bottom panels highlight possible colocalization between ATAD3 and STAT3.

Indeed, the proliferation rate in the TPZ of 48-hpf embryos injected with *MLS_mStat3_NES_S727A* mRNA resulted significantly lower to that of embryos injected with the WT form (Fig. 6 A,B). However, a mild although significant increase of *pcna* was detectable in embryos injected with *MLS_mStat3_NES_S727A* mRNA when compared to non-injected controls, meaning that part of the mitochondrial functions might be conserved even in the absence of S727 phosphorylation (Fig. 6 B).

In mouse 3T3 fibroblasts the MEK-ERK pathway is known to be responsible for STAT3 S727 phosphorylation (Gough *et al.*, 2013). In order to evaluate *in vivo* the involvement of MEK-ERK pathway in STAT3 S727 phosphorylation, and the downstream effects for mitoSTAT3-driven cell proliferation, we administered a specific inhibitor of MEK kinases PD98059 (Alessi *et al.*,1995) commonly used *in vitro* to prevent specifically S727 phosphorylation on STAT3 (Tian and Al., 2004; Wang *et al.,* 2019). After treatment from 24-48 hpf to WT embryos injected with *MLS_Stat3_NES* and evaluated the relative cell proliferation rate by immune fluorescence using anti Phospho-Histone H3 (pH3) Antibody (Fig. 6C; Fig. S3). Notably, the increase in the number of proliferating cells in the head

after injection with *MLS_Stat3_NES* was abolished by treatment with PD98059 (Fig. 6 C; Fig. S3). Moreover, while a significant difference in the number of pH3-expressing cells occurred between embryos injected with *MLS_Stat3_NES* and *MLS_mStat3_NES_S727A,* such difference was not maintained after PD98059 treatment (Fig. 6 C; Fig. S3). All together these results demonstrate that the MEK-ERK pathway is directly responsible for the phosphorylation of STAT3 on S727 residue, thus enabling mitoSTAT3 induced cell proliferation.

Jak2 kinase maintains normal mtDNA transcription and proliferation in the PML and the intestine

After demonstrating that a) mitoSTAT3 driven mitochondrial transcription relies on both

14

Y705 and S727 post-transcriptional phosphorylation, and b) that the consequential proliferation effect downstream of mitochondrial transcription requires functional ERK(MAPK) kinases, we decided to test the dependence of both mitochondrial transcription and cell proliferation on Jak2 Tyrosine-kinase activity. WT embryos were therefore treated from 24 to 72 hpf with AG490, a specific inhibitor of Jak2 widely used as a JAK/STAT3 inhibitor (Park *et al.,* 2014; Garbuz *et al.,* 2014) and the expression of *mt_nd2* was assessed by qRT-PCR. When observed at 72 hpf, AG490-treated larvae displayed a significant reduction of *mt_nd2* expression in the PML, the inner retina and the primordium of the intestine (Fig. 7 A (arrowheads)), while no significant decrease was present at 48 hpf. (Fig. 7 B). In addition, proliferation activity was found to be significantly reduced in the TPZ of 72-hpf AG490-treated larvae as assayed by *in situ* hybridization using anti-*pcna* probe (Fig. 7 C, D).
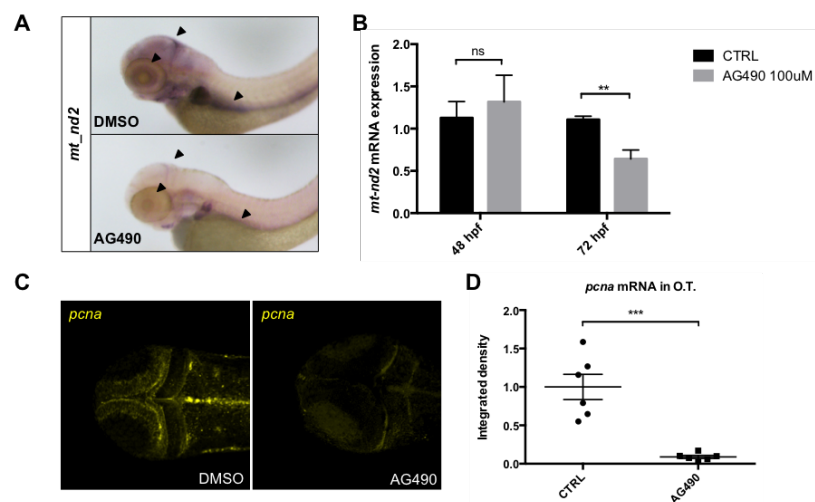
Fig. 7 **Jak2 inhibition impairs normal mitochondrial transcription and cell proliferation in the TeO of 72-hpf embryos.** A: WISH with anti-*mt_nd2* mRNA probe on 72-hpf embryos treated with 100 μM AG490 from 24-72 hpf and DMSO treated controls. B: relative *mt_nd2* transcript expression assayed by qRT-PCR in 48- and 72-hpf embryos treated with 100 μM AG490 and DMSO treated controls starting from 24 hpf; *zgapdh* was used as internal control (p-values= 0,6261; 0,0060). C: FISH with anti-*pcna* probe in the TeO of 72-hpf embryos treated with 100 μM AG490 from 24 to 72 hpf and DMSO treated controls. D: Fluorescence quantification of *pcna* mRNA expression in the TeO (n=6) (p-value=0,0003). Statistical analysis was performed by unpaired t-test on 3 independent biological samples (where n not specified)*. ns: not significant; **p<0,01; ***p<0.001; error bars=SEM.

We also investigated the effect of Jak2 inhibitor in the intestine, a highly proliferating tissue of zebrafish larvae, where *mt_nd2* gene is strongly expressed between 3 and 6 dpf (Fig. 8A). The activity of Stat3 in the intestine of zebrafish is consistent with the facts that a) the

15

proliferative and survival effects of IL-6 in murine IECs (intestinal epithelial cells) is largely mediated by STAT3 (Grivennikov *et al.*, 2009), b) that STAT3 is needed for small-intestine crypt stem cell survival, as revealed by conditional mutant mice (Matthews *et al.*, 2011), and c) that Stat3 positive cells in zebrafish intestine represent a population of intestinal Wnt responsive stem cells (Peron *et al.*, 2020). Administration of 60 µM AG490 between 3 and 6 dpf was able to significantly reduce mitochondrial transcription in the intestine of treated larvae with respect to DMSO treated controls (Fig. 8 A, B). Moreover, the treatment of larvae with AG490 caused a significant decrease in the number of intestinal proliferating cells (revealed by immunohistochemistry with anti-pH3 antibody) (Fig. 8 C, D) and resulted in flattening of the intestinal mucosa (Fig. 8 E, F). Taken all together, these experiments demonstrate for the first time *in vivo* that phosphorylation of the Stat3 Y705 residue, possibly by enabling import of Stat3 into mitochondria, is required in zebrafish for normal mitochondrial transcription and downstream proliferation in the developing TeO and intestine.
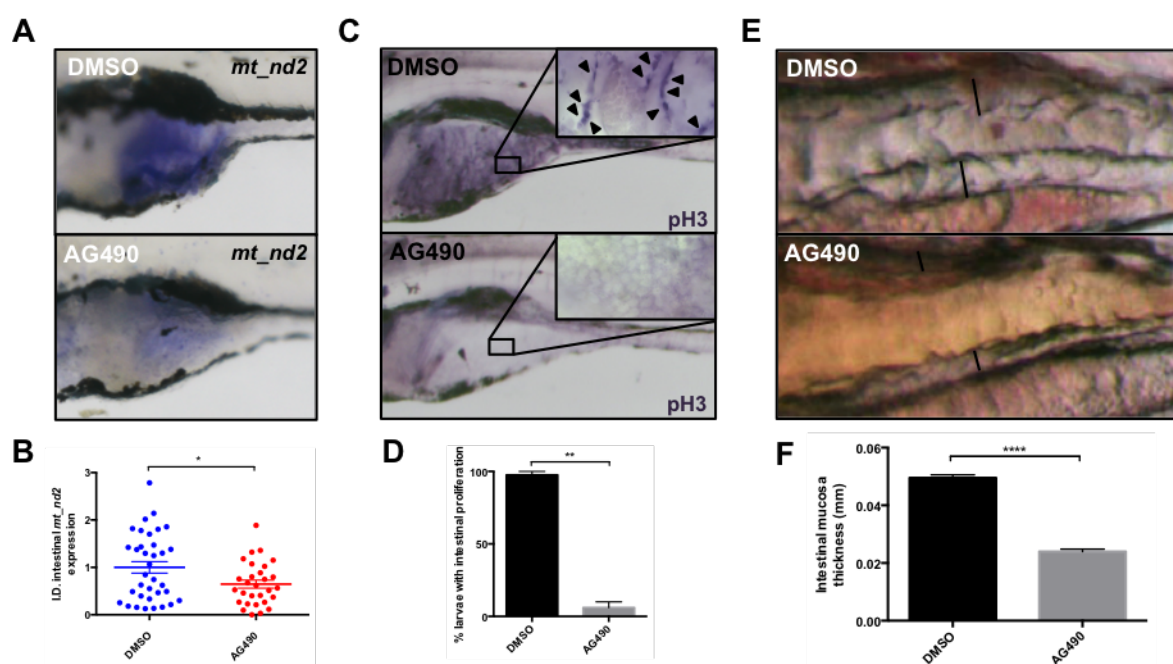
Fig.8 **Jak2 inhibition impairs normal mitochondrial transcription and cell proliferation in the intestine of 6-dpf larvae.** A: WISH with anti-*mt_nd2* mRNA probe on 6-dpf larvae treated with 60 µM AG490 from 24-72 hpf and DMSO treated controls; zoom on the intestine. B: Quantification of *mt_nd2* mRNA expression in the intestine (n=30) (p-value= 0,0240). C: phospho-Histone-H3 (pH3) immunostaining of 6-dpf AG490 treated larvae and DMSO treated controls; zoom on the intestine; (pH3 positive cells=arrowheads). D: Quantification of the number of AG490 and DMSO treated larvae displaying intestinal proliferation (n=15) (p-value= 0,0026). E: AG490 treated larvae showing loss of folding in intestinal mucosa. F: Graph showing the dimension of mucosal thickness in both DMSO and AG490 6-dpf treated

larvae (n=18) (p-value= 0,0001). Statistical analysis was performed by unpaired t-test on indicated number of samples; *p<0,05; **p<0,01; ***p<0.001; error bars=SEM.

The zebrafish *stat3⁻/⁻* null mutant displays impairment of mitochondrial transcription and cell proliferation in CNS and intestine

To confirm data obtained by endogenous Stat3 chemical treatment with either MEK and Jak2 inhibitors, we used the *stat3^{ia23}* mutant (from now on called *stat3⁻/⁻*) (Peron *et al*., 2020), which is predicted to encode a premature stop codon at amino acid 456, thus lacking all functional domains including the dimerization domain and the transactivation domain, harboring Y705 and S727 phosphorylation sites, respectively. Consistently with our previous results, Stat3 genetic ablation caused a significant and clear reduction of both *mt_nd2* and *pcna* transcripts, endorsing the link between Stat3 mitochondrial functions and its role in regulating cell proliferation in different tissues. Notably, about 70% of *stat3⁻/⁻* larvae display severe defects in the development of intestinal epithelium (Peron *et al*., 2020): as revealed by pHH3 immunostaining, intestinal mitoses are almost absent (Fig. 8 B-B') and the intestine fails to fold (Fig. 9 C-C'). These phenotypic alterations are almost identical to those induced by AG490 treatment (Fig. 7 B,C). At 6 dpf *stat3⁻/⁻* larvae also show impaired CNS cell proliferation in the Telencephalon (Tel), the Diencephalon (Di) and the TeO, where Pcna is found to be reduced down to 15% with respect to wild-type, supporting, once again, the requirement of Stat3 to maintain normal proliferation in the brain (Fig. 9 D, E).

Interestingly, no overt structural alteration is present in intestinal or brain mitochondria of 6-dpf *stat3⁻/⁻* larvae analysed by Transmission Electron Microscopy (TEM) (Fig. S4 A). Moreover, in order to evaluate the amount of mitochondria, we crossed *stat3* mutants with

17
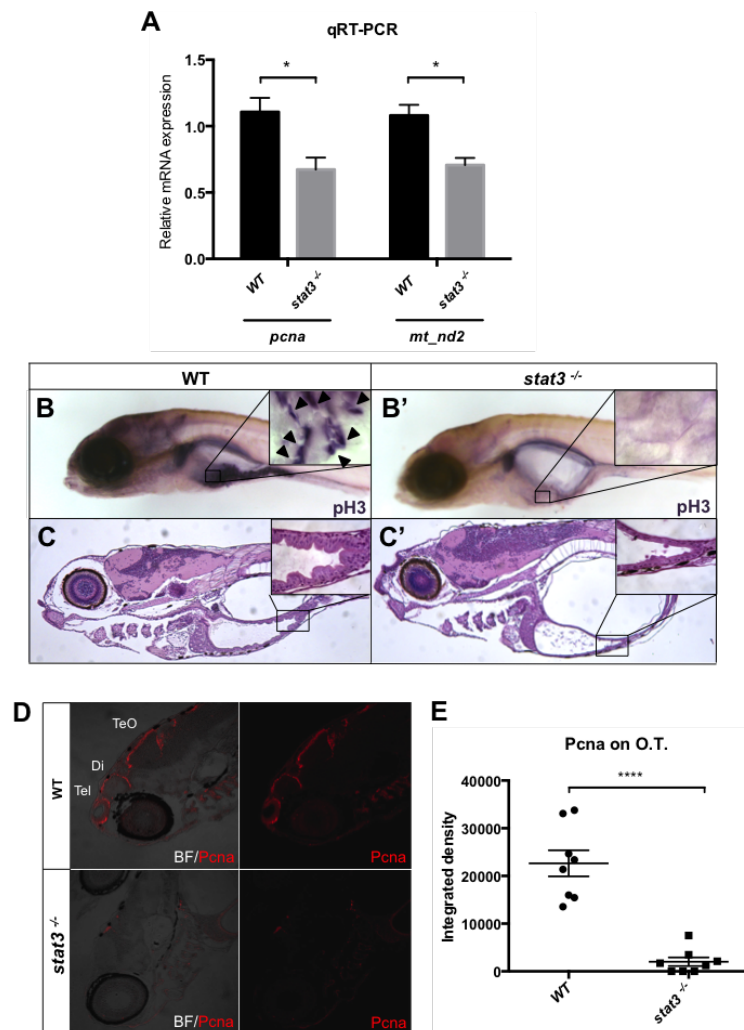
Fig. 9 **stat3 KO impairs normal mitochondrial transcription and cell proliferation in the intestine and brain of 6-dpf zebrafish larvae.** A: Relative mRNA expression of *mt_nd2* and *pcna* transcripts assayed by qRT-PCR in homogenized *stat3$^{-/-}$* and WT siblings at 6 dpf; *zgapdh* was used as internal control (p-values= 0,0358; 0,0182). B-B': phospho-Histone-H3 (pH3) immunostaining of *stat3$^{-/-}$* and WT siblings at 6 dpf; zoom on the intestine. (pH3 positive cells=arrowheads). C-C': EE staining on WT and *stat3$^{-/-}$* mutant sections at 6 dpf shows the complete loss of folding in the mutant intestinal epithelium. D: IF with anti-PCNA Ab on 6-dpf *stat3$^{-/-}$* mutants showing decrease of fluorescence in the CNS (Tel= telencephalon; Di: diencephalon; TeO: tectum opticum). E: Fluorescence quantification of PCNA protein on lateral sections of 6-dpf *stat3$^{-/-}$* mutants and WT siblings; zoom on the head (n=8) (p-value<0,0001). Statistical analysis was performed by unpaired t-test on 3 independent biological samples (where n not specified). *p<0,05; ****p<0,0001; error bars=SEM.

the *Tg(CoxVIII-mls:EGFP)* transgenic line that expresses a mitochondria- localized form of enhanced GFP. No clear change in the total mitochondria volume was present in the intestine of *stat3$^{-/-}$* larvae with respect to WT (Fig. S4 B,C). Together with previous results, this highlights that mitoSTAT3 is only acting as regulator of mitochondrial transcription, without impacting on mitochondria biogenesis or homeostasis.

18

DISCUSSION

Using zebrafish and taking advantage of a STAT3 harbouring both a mitochondrial localization sequence and a nuclear export signal, we tried to figure out how mitoSTAT3 may act inside the mitochondrion. Interestingly, since mitochondrial mRNAs a) are reduced in *stat3*^{ia23/ia23} zebrafish null mutants b) are decreased in embryos treated with the Jak2 kinase inhibitor AG490 and c) the effect of *MLS_Stat3_NES* in promoting mitochondrial gene expression is abolished by Balapiravir (a mtRNApol inhibitor), our data strongly support, *in vivo*, a direct link between mitoSTAT3 activity and mitochondrial transcription. This is consistent with the mitochondrial transcriptional role of mitoSTAT3 found *in vitro* in murine ESC by Carbognin and colleagues (Carbognin *et al.*, 2016). On the other hand, quite surprisingly for a transcription factor, *MLS_Stat3_NES* mutated in its DNA-binding domain is still able to increase mitochondrial transcription. This result suggests that STAT3, differently from what hypothesized in Macias *et al*. (2014), does not regulate mtDNA transcription by binding STAT3 responsive elements located in the mtDNA. One of the most fascinating aspects of mitochondria evolution is their progressive incorporation in the machinery of cell regulatory activities such as cell proliferation and apoptosis (Antico Arciuch *et al.,* 2012). By showing that mitoSTAT3-driven mitochondrial transcription controls cell proliferation, at least in intestinal and tectal udifferentiated progenitor cells, our data partially answer the open questions about the mechanisms that synchronize mitochondrial and nuclear activities during cell proliferation.

Canonical STAT3 activation depends on different modifications, such as the phosphorylation at tyrosine 705 (Y705), that induces dimerization and translocation to the nucleus, and at serine 727 (S727), whose function has been reported to have controversial effects on STAT3 nuclear transcriptional activity (Decker *et al.*, 2000; Huang *et al.*, 2014). On the other hand, the post-translational modifications required for mitoSTAT3 import and activity in mitochondria have not been clearly dissected so far, although phosphorylation at S727 has been found to both activate OXPHOS complexes I and II, and suppress ROS production and cytochrome c release following ischemic injury (Meier & Larner, 2014). More recently STAT3 phosphorylation at S727 was also found to be required for STAT3-mediated regulation of ER Ca^{2+} fluxes and apoptosis through the regulation of the mitochondrial Ca2+ uptake (Avalle *et al.,* 2019). We provide here *in vivo* evidence that phosphorylation of STAT3 Y705, being required for precise mitochondrial import of STAT3, is needed for STAT3-mediated mitochondrial gene expression. In addition, in accordance with Wegrzyn *et al.*

(2009), we show that mitochondrial STAT3 transcriptional activity *in vivo* is totally dependent on phosphorylation of the ERK target S727. Notably, it has been shown that loss of S727 phosphorylation causes a significant reduction of neuronal differentiation potential, demonstrating the role of this post-translational modification in determining cell pluripotency and proliferation (Huang *et al.*, 2014). In agreement, while we see no effect in the expression of neural progenitor cells markers upon mitoSTAT3 overexpression, our results show that both mitoSTAT3-mediated mtDNA transcription and cell proliferation can be repressed by targeting S727 with the MEK (kinase of ERK1/2 protein kinase) specific inhibitor PD98059. All in all, our results add new knowledge about the role of mitochondrial STAT3 in the regulation of cellular processes previously thought to be dependent exclusively on canonical STAT3. Together with the fact that mitochondrial STAT3 has been identified as a contributor to RAS-dependent cellular transformation (Gough *et al.*, 2009), we support the idea of ERK-mitoSTAT3-mediated mitochondrial transcription might be a key process in cancer development. Considering that, to date, the vast majority of STAT3-targeted cancer therapeutic approaches focus only on its canonical functions, our findings imply mitochondrial STAT3-specific transcriptional activity as a significant molecular mechanism to be targeted.

MATERIALS AND METHODS

Animal husbandry and lines

Animals were staged and fed as described by Kimmel *et al.* (1995) and maintained in large scale aquaria systems.

Embryos were obtained by natural mating, raised at 28 °C in Petri dishes containing fish water (50X: 25 g Instant Ocean, 39.25 g $CaSO_4$ and 5 g $NaHCO_3$ for 1 L) and kept in a 12:12 light-dark (LD) cycle. All experimental procedures complied with European Legislation for the Protection of Animals used for Scientific Purposes (Directive 2010/63/EU).

stat3[ia23] mutants are described in Peron *et al*. (2020). *Tg(CoxVIII-mls:EGFP)* transgenic zebrafish line is described in Martorano *et al.* (2019).

Drug treatments

The following chemical compounds were used: AG490 (T3434, Sigma Aldrich); PD98059 (PHZ1164, Thermo Fisher Scientific); Balapiravir (HY-10443, DBA). Before drug administration, a hole was made in the chorion of 8 hpf embryos, while 24 hpf embryos were dechorionated. All drugs were dissolved in DMSO and stored in small aliquots at -20°C. 100 µM AG490 treatment was performed from 24 to 48 hpf or from 24 to 72 hpf. 60 µM AG490 was administrated in 3-6 dpf treatments. 12.5 µM PD98059 treatment was administrated from 24 to 48 hpf. 50 µM Balapiravir solution was administrated from 8 to 48 hpf. After treatments, embryos were either anesthetized and fixed in 4% paraformaldehyde (PFA)(158127, Sigma) in PBS for ISH, FISH and IHC or in TRI Reagent® (T9424, Sigma) for qRT-PCR analysis.

mRNAs synthesis and injection

mStat3, *mStat3_Y705F* and *mStat3_S727A* CDSs were obtained from pCEP4-*Stat3-WT*, pCEP4-*Stat3-Y705F*, pCEP4-*Stat3-S727A* plasmids (a kind gift of the Poli Lab; Department of Molecular Biotechnology and Health Sciences, Molecular Biotechnology Center, University of Turin) and sub-cloned into a pCS2+ backbone using the In-Fusion® HD Cloning Kit (Clonetech). *MLS_mStat3_NES* CDS, containing the murine *Stat3* cDNA flanked by a Mitochondrial Localization Sequence (MLS) and a Nuclear Export Sequence (NES), was subcloned into a pCS2+ plasmid from a 70_pPB-CAG+MLS+*Stat3*+NES-pA-pgk-hph-2-2 plasmid by digestion with XbaI and BamHI. Mutated forms of *MLS_mStat3_NES* mRNA

21

were obtained from pCS2+*MLS_mStat3_NES* by site directed mutagenesis using the Q5® Site-Directed Mutagenesis Kit (NEB); primers are indicated in Table 1.

mRNAs were *in vitro* transcribed using the mMESSAGE mMACHINE® SP6 Transcription Kit (Thermo Fisher Scientific) and purified using the RNA Clean and Concentrator kit (Zymo Research). A mix containing mRNA (30 ng/µL for *Stat3-WT, Stat3-Y705F, Stat3-S727A*; 50 ng/µL for *MLS_Stat3_NES*), Danieu injection Buffer and Phenol Red injection dye, was injected into 1-cell stage embryos.

Table 1.

Primer name	Primer sequence
MLS_STAT3_NES_Y705F fw	GCTGCCCCGTTCCTGAAGACC
MLS_STAT3_NES_Y705F rv	ACTACCTGGGTCGGCTTC
MLS_STAT3_NES_S727A fw	CCTGCCGATGGCCCCCCGCAC
MLS_STAT3_NES_S727A rv	TCAATGGTATTGCTGCAGGTCGTTGGTGTC
MLS_STAT3_NES_ΔDNAbd fw	GGCGATCTCCAACATCTGTCAGATGC
MLS_STAT3_NES_ΔDNAbd rv	GCGGCTGGCAAGGAGTGGGTCTC

mRNA isolation and quantitative real time reverse transcription PCR (qRT-PCR)

For expression analysis, total RNA was extracted from pools of 15 7-dpf larvae or 35 48-hpf embryos with TRIzol reagent (Thermo Fisher Scientific, 15596018). mRNA was treated with RQ1 RNase-Free DNase (Promega, M6101) and then used for cDNA synthesis with Superscript III Reverse Transcriptase (Invitrogen, 18080-044) according to the manufacturer's protocol. qPCRs were performed in triplicate with EvaGreen method using a Rotor-gene Q (Qiagen) and the 5x HOT FIREPol ® EvaGreen® qPCR Mix Plus (Solis BioDyne, 08-36-00001) following the manufacturer's protocol. The cycling parameters were: 95 °C for 14 min, followed by 45 cycles at 95 °C for 15 s, 60 °C for 35 s, and 72°C for 25 s. Threshold cycles (Ct) and dissociation curves were generated automatically by Rotor-Gene Q series software. Sequences of specific primers used in this work for qRT-PCR and RT-PCR are listed in Table 2. Primers were designed using the software Primer 3 (http://bioinfo.ut.ee/primer3-0.4.0/input.htm). Sample Ct values were normalized with Ct values from zebrafish *gapdh*.

Table 2.

Gene	Forward primer sequence	Reverse primer sequence
zmt_nd2	GCAGTAGAAGCCACCACAAA	GCTAGACCGATTTTGAGAGCC
zgapdh	GTGGAGTCTACTGGTGTCTTC	GTGCAGGAGGCATTGCTTACA
zpcna	CCTTGGCACTGGTCTTTGAA	GGCACACGAGATCATGACAG
zsocs3a	GGAAGACAAGAGCCGAGACT	GCGATACACACCAAACCCTG
mSocs3	ATTTCGCTTCGGGACTAGC	AACTTGCTGTGGGTGACCAT
mStat3	TGTTGGAGCAGCATCTTCAG	GAGGTTCTCCACCACCTTCA
mbactin	CTAAGGCCAACCGTGAAAAG	ACCAGAGGGCATACAGGGACA

Immunoblotting and mitochondria isolation

Immunoblotting was performed as previously described in Carbognin *et al.* (2016). Following antibodies were used: anti-STAT3 mouse monoclonal (Cell Signalling, 9139) (1:1000), anti-GAPDH mouse monoclonal (Millipore, MAB374) (1:1000), anti-VDAC1 rabbit polyclonal (abcam, ab15895) (1:1000), anti-Lamin () (1:1000), anti-bActin mouse monoclonal (Invitrogen, MA1-744) (1:10000). Mitochondria from mouse ESCs were isolated using Mitochondria isolation kit (Thermo Scientific, 89874).

3,3'-Diaminobenzidine staining

Cells were fixed in a 24 wells plate with 4% Paraformaldehyde in PBS (pH 7,4) for 30 minutes at RT (room temperature). After fixation cells were washed 5 times with PBS (5 minutes each), blocked and permeabilized with 5% normal goat serum and 0,1% saponin in PBS for 30 min, and then incubated with primary antibody anti-STAT3 mouse monoclonal (Cell Signalling, 9139) ON at 4°C in PBS 5% normal goat serum and 0,05% saponin. After 5 washes with PBS (5 minutes each), cells were incubated with HRP-conjugated Fab fragments of the secondary antibody for 2 hours at RT. After 5 washes, cells were incubated in the DAB solution (0.01gr DAB in 20ml TRIS-HCl buffer plus 30% H_2O_2 solution just before use). Subsequently the samples ware postfixed with 1% osmium tetroxide plus potassium ferrocyanide 1% in 0.1M sodium cacodylate buffer for 1 hour at 4°C. After three water washes, samples were dehydrated in a graded ethanol series and embedded in an epoxy resin (Sigma-Aldrich). Ultrathin sections (60-70 nm) were obtained with an Ultrotome V (LKB) ultramicrotome, counterstained with uranyl acetate and lead citrate and viewed with a Tecnai G2 (FEI) transmission electron microscope operating at 100 kV. Images were captured with a Veleta (Olympus Soft Imaging System) digital camera.

Immunofluorescence

ES cells were grown and transfected as described by Carbognin *et al.* (2016). For IF ESCs were fixed for 10 min in cold methanol at −20 °C, washed in TBS, permeabilized for 10 min with TBST + 0.3% Triton X-100 at RT, and blocked for 45 min in TBS + 3% goat serum at RT. The cells were incubated overnight at 4 °C with primary antibodies (anti-STAT3 mouse monoclonal (Cell Signalling, 9139) (1:100); anti-ATAD3A rabbit monoclonal (AB-Biotechnologies, 224485) (1:100). After washing with TBS, the cells were incubated with secondary antibodies (Alexa, Life Technologies) for 30 min at RT. Cells were mounted with ProLong® Gold Antifade Mountant with DAPI (Life Technologies, cat. P36941) or HOECHST 33342 (Thermo Fisher cat. 62249) where specifield. Images were acquired with a Leica SP2 confocal microscope equipped with a CCD camera.

In situ hybridization

Whole mount RNA in situ hybridization on zebrafish embryos was performed as previously described (Thisse *et al.*, 1993). It is worth mentioning that treated and control embryos were hybridized together. *stat3* probe was obtained by PCR amplification from embryos cDNA using *stat3*_probe-fw (TGCCACCAACATCCTAGTGT) and *stat3*_probe-rv (GCTTGTTTGCACTTTTGACTGA) primers. *mt_nd2* probe was obtained by PCR amplification from embryos cDNA using *mt_nd2*-fw (GCAGTAGAAGCCACCACAAA) and *mt_nd2*-rv (GGAATGCCGCGGATGTTATA) primers. *pcna* probe was obtained as described by Baumgart *et al.* (2014). *sox9b* probe was obtained as described by Chiang *et al.* (2001). *her5* probe was obtained as described by Bally-Cuif, *et al.* (2000). *her4* probe was obtained as described by Takke *et al.* (1999). Fluorescence in situ hybridization was performed with FastBlue or TSA-amplification kit (Invitrogen) as described by Lauter *et al.* (2011).

Transmission Electron Microscopy analysis

Larvae were anesthetised and fixed with 2.5% glutaraldehyde in 0.1 M sodium cacodylate buffer. After that, samples were dehydrated, embedded in epoxy resin, and prepared according standard protocols by the Trasmission Electron Microscopy facility at the Department of Biology (University of Padova).

Statistical analysis

Statistical analysis was performed with Graph Pad Prism V6.0. Data are presented as the means ± SEM and statistical analysis was determined by unpaired two tailed Student's t-test. The p-values are indicated with the following symbols: *, P<0.05; **, P<0.01; ***, P< 0.001; ****, P<0.0001. For quantitative analysis, the sample size for each experiment was calculated assuming a Confidence Level of 95% (z-score 1,96), a standard deviation of 0.5 and a Confidence Interval (margin of error) of 5%.

Acknowledgments

Competing interests

The authors declare no competing or financial interests.

REFERENCES

Alessi D.R., Cuenda A., Cohen P., Dudley D.T., Saltiel A.R. (1995). PD 098059 is a specific inhibitor of the activation of mitogen-activated protein kinase kinase in vitro and in vivo. *J Biol Chem.* **270(46):**27489-94.

Antico Arciuch VG, Elguero ME, Poderoso JJ, Carreras MC. (2012). Mitochondrial regulation of cell cycle and proliferation. *Antioxid Redox Signal.* **16(10)**:1150-80.

Avalle L., Camporeale A., Morciano G., Caroccia N., Ghetti E., Orecchia V., Viavattene D., Giorgi C., Pinton P., Poli V. (2019). STAT3 localizes to the ER, acting as a gatekeeper for ER-mitochondrion Ca2+ fluxes and apoptotic responses. Cell Death Differ. May;26(5):932-942.**Bally-Cuif, L., Goutel, C., Wassef, M., Wurst, W., & Rosa, F.** (2000). Coregulation of anterior and posterior mesendodermal development by a hairy-related transcriptional repressor. *Genes & development.* **14(13),** 1664-77.

Baumgart, M., Groth, M., Priebe, S., Savino, A., Testa, G., Dix, A., Ripa, R., Spallotta, F., Gaetano, C., Ori, M., Terzibasi Tozzini, E., Guthke, R., Platzer, M. and Cellerino, A. (2014). RNA-seq of the aging brain in the short-lived fish N. furzeri – conserved pathways and novel genes associated with neurogenesis. *Aging Cell.* **13**: 965–974.

Becker S., Groner B., Müller C.W. (1998). Three-dimensional structure of the Stat3beta homodimer bound to DNA. *Nature.* **394:**145–151 10.1038/28101

Burdon T, Chambers I, Stracey C, Niwa H, Smith A. (1999). Signaling mechanisms regulating self-renewal and differentiation of pluripotent embryonic stem cells. *Cells Tissues Organs.* **165(3-4):**131-43.

Carbognin, E., Betto, R. M., Soriano, M. E., Smith, A. G. and Martello, G. (2016). Stat3 Promotes Mitochondrial Transcription and Oxidative Respiration during Maintenance and Induction of Naive Pluripotency. *EMBO J.* **35,** 618-634.

Chiang E.F.L., Pai C.I., Wyatt M., Yan Y.L, Postlethwait J, and Chung B.C (2001). Two sox9 genes on duplicated zebrafish chromosomes: Expression of similar transcription activators in distinct sites. *Dev Bio.* **231**: 149-163.

Decker T., & Kovarik P. (2000). Serine phosphorylation of STATs. *Oncogene.* **19**: 2628–2637.

Feng JY, Xu Y, Barauskas O, Perry JK, Ahmadyar S, Stepan G, Yu H, Babusis D, Park Y, McCutcheon K, Perron M, Schultz BE, Sakowicz R, Ray AS. (2015) Role of Mitochondrial RNA Polymerase in the Toxicity of Nucleotide Inhibitors of Hepatitis C Virus. *Antimicrob Agents Chemother.* **60(2):**806-17.

Fouse, S.D., Costello, J.F. (2013). Cancer Stem Cells Activate STAT3 the EZ Way. *Cancer*

Cell. **23(6).** 711–713.

Gagnon, J.A., Valen, E., Thyme, S.B., Huang, P., Ahkmetova, L., Pauli, A., et al. (2014). Efficient Mutagenesis by Cas9 Protein-Mediated Oligonucleotide Insertion and Large-Scale Assessment of Single-Guide RNAs. *PLoS ONE.* **9(5):** e98186.

Galant, S., Furlan, G., Coolen, M., Dirian, L., Foucher, I., & Bally-Cuif, L. (2016). Embryonic origin and lineage hierarchies of the neural progenitor subtypes building the zebrafish adult midbrain. *Developmental biology.* **420(1)**, 120-135.

Ghoshal, S., Fuchs, B. C., & Tanabe, K. K. (2016). STAT3 is a key transcriptional regulator of cancer stem cell marker CD133 in HCC. *Hepatobiliary Surgery and Nutrition.* **5(3)**, 201–203.

Gough D.J., Corlett A., Schlessinger K., Wegrzyn J., Larner A.C., Levy DE. (2009). Mitochondrial STAT3 supports Ras-dependent oncogenic transformation. *Science.* **324(5935)**:1713-6.

Gough DJ, Koetz L, Levy DE. (2013) The MEK-ERK Pathway Is Necessary for Serine Phosphorylation of Mitochondrial STAT3 and Ras-MediatedTransformation. *PLoS ONE* 8(11): e83395.

Grivennikov, S., Karin, E., Terzic, J., Mucida, D., Yu, G. Y., Vallabhapurapu, S., Scheller, J., Rose-John, S., Cheroutre, H., Eckmann, L. et al. (2009). IL-6 and Stat3 are Required for Survival of Intestinal Epithelial Cells and Development of Colitis-Associated Cancer. *Cancer. Cell.* **15,** 103-113.

Gurbuz V., Konac E., Varol N., Yilmaz A., Gurocak S., Menevse S., Sozen S. (2014). Effects of AG490 and S3I-201 on regulation of the JAK/STAT3 signaling pathway in relation to angiogenesis in TRAIL-resistant prostate cancer cells in vitro. *Oncol Lett.* **7(3):** 755–763.

Horvath C M, Wen Z, Darnell J E., Jr. (1995). A STAT protein domain that determines DNA sequence recognition suggests a novel DNA-binding domain. *Genes Dev.* **9:**984–994.

Huang, G., Yan, H., Ye, S., Tong, C., Ying, Q.L. (2014). STAT3 phosphorylation at tyrosine 705 and serine 727 differentially regulates mouse ESC fates. *Stem Cells.* **32**:1149–1160.

Jo, A., Denduluri, S., Zhang, B., Wang, Z., Yin, L., Yan, Z., Kang, R., Shi, L. L., Mok, J., Lee, M. J., … Haydon, R. C. (2014). The versatile functions of Sox9 in development, stem cells, and human diseases. *Genes & diseases.* *1(2),* 149-161.

Johnston PA, Grandis JR. (2011). STAT3 signaling: anticancer strategies and challenges. *Mol Interv.* **11(1):**18-26.

Kimmel, C. B., Ballard, W. W., Kimmel, S. R., Ullmann, B. and Schilling, T. F. (1995), Stages of embryonic development of the zebrafish. *Dev. Dyn.* **203**: 253–310.

Klüver, N., Kondo, M., Herpin, A., Mitani H., Schartl M. (2005). Divergent expression patterns of *Sox9* duplicates in teleosts indicate a lineage specific subfunctionalization. *Dev Genes Evol.* **215**:297.

Lauter, G., Söll, I., & Hauptmann, G. (2011). Two-color fluorescent in situ hybridization in the embryonic zebrafish brain using differential detection systems. *BMC developmental biology*. **11,**43.

Liu Y., Sepich D.S., Solnica-Krezel L. (2017) Stat3/Cdc25a-dependent cell proliferation promotes embryonic axis extension during zebrafish gastrulation. *PLoS Genet.* **13(2):** e1006564. https://doi.org/10.1371/journal.pgen.1006564

Macias, E., Rao, D., Carbajal, S., Kiguchi, K. and DiGiovanni, J. (2014). Stat3 Binds to mtDNA and Regulates Mitochondrial Gene Expression in Keratinocytes. *J. Invest. Dermatol.* **134,** 1971-1980.

Mantel, C., Messina-Graham, S., Moh, A., Cooper, S., Hangoc, G., Fu, X. Y., & Broxmeyer, H. E. (2012). Mouse hematopoietic cell-targeted STAT3 deletion: stem/progenitor cell defects, mitochondrial dysfunction, ROS overproduction, and a rapid aging-like phenotype. *Blood.* **120(13)**, 2589-99.

Martello G., Bertone P., Smith A. (2013) Identification of the missing pluripotency mediator downstream of leukaemia inhibitory factor. *EMBO J.* 32(19):2561-74.

Martini S., Bernoth K., Main H., Ortega G.D., Lendahl U., Just U., Schwanbeck R. (2013). A critical role for Sox9 in notch-induced astrogliogenesis and stem cell maintenance. *Stem Cells.* **31:**741–751.

Martorano L., Peron M., Laquatra C., Lidron E., Facchinello N., Meneghetti G., Tiso N., Rasola A., Ghezzi D., Argenton F. (2019) The zebrafish orthologue of the human hepatocerebral disease gene *MPV17* plays pleiotropic roles in mitochondria. *Dis Model Mech.* **12(3):** dmm0372226.

Matsuda T., Nakamura T., Nakao K., Arai T., Katsuki M., Heike T., Yokota T. (1999). STAT3 activation is sufficient to maintain an undifferentiated state of mouse embryonic stem cells. *EMBO J*. **18(15):**4261-9.

Matthews J. R., Sansom O. J. and Clarke A. R. (2011). Absolute Requirement for STAT3 Function in Small-Intestine Crypt Stem Cell Survival. *Cell Death Differ.* **18,** 1934-1943.

Meier, J. A., & Larner, A. C. (2014). Toward a new STATe: the role of STATs in mitochondrial function. *Seminars in immunology*, **26**(1), 20-8.

Ni C., Hsieh H., Chao Y., Wang D.L. (2004). Interleukin-6-induced JAK2/STAT3 signaling pathway in endothelial cells is suppressed by hemodynamic flow. *American Journal of Physiology. Cell Physiology.* **287**(3) C771-C780.

28

Oates A. C., Wollberg P., Pratt S. J., Paw B.H., Johnson S. L., Ho R. K., PostIrthwait J. H., Zon L. I., Wilks A. F. (1999). Zebrafish stat3 is expressed in restricted tissues during embryogenesis and stat1 rescues cytokine signaling in a STAT1-deficient human cell line. *Dev Dyn*. **215**:352–370.

O'Shea J.J., Schwartz D.M., Villarino A.V., Gadina M., McInnes I.B., Laurence A. (2015). The JAK-STAT pathway: impact on human disease and therapeutic intervention. *Annu Rev Med.* **66**:311-28.

Park J.S., Lee J., Lim M.A., Kim E.K., Kim S.M., Ryu J.G., Lee J.H., Kwok S.K., Park K.S., Kim H.Y., Park S.H., Cho M.L. (2014) JAK2-STAT3 blockade by AG490 suppresses autoimmune arthritis in mice via reciprocal regulation of regulatory T Cells and Th17 cells. J Immunol. May 1;192(9):4417-24.

Peron M., Dinarello A., Meneghetti G., Martorano L., Facchinello N., Vettori A., Licciardello G., Tiso N., Argenton F. (2020) The stem-like STAT3-responsive cells of zebrafish intestine are WNT/β-catenin dependent. *Development*. **147(12):** dev188987

Qin, H.R., Kim H.J., Kim J.Y., Hurt E.M., Klarmann G.J., Kawasaki B.T., Duhagon Serrat M.A., … Farrar W.L. (2008). Activation of signal transducer and activator of transcription 3 through a phosphomimetic serine 727 promotes prostate tumorigenesis independent of tyrosine 705 phosphorylation. *Cancer research*. **68(19)**, 7736-41.

Scott C.E., Wynn S.L., Sesay A., Cruz C., Cheung M., Gomez Gaviro M.V., Booth S., Gao B., Cheah K.S., Lovell-Badge R., Briscoe J. (2010) SOX9 induces and maintains neural stem cells. *Nat Neurosci.* **13:**1181–1189.

Shi X., Zhang H., Paddon H., Lee G., Cao X., Pelech S. (2006). Phosphorylation of STAT3 serine-727 by cyclin-dependent kinase 1 is critical for nocodazole-induced mitotic arrest. *Biochemistry*. **45**:5857–5867.

Szczepanek K., Chen, Q., Derecka M., Salloum F.N., Zhang Q., Szelag M., Cichy J., Kukreja R.C., Dulak J., Lesnefsky E.J., *et al.* (2011). Mitochondrial-targeted signal transducer and activator of transcription 3 (stat3) protects against ischemia-induced changes in the electron transport chain and the generation of reactive oxygen species. *J. Biol. Chem.* **286**,29610–29620.

Taanman, J. (1999). The mitochondrial genome: structure, transcription, translation and replication. *Biochimica et Biophysica Acta-Bioenergetics.* **1410(2),** 103-123.

Takke C., Dornseifer P., v Weizsäcker E., Campos-Ortega J.A. (1999). her4, A zebrafish homologue of the Drosophila neurogenic gene E(spl), is a target of NOTCH signalling. *Development.* **126**: 1811–1821.

Thisse B., Pflumio S., Fürthauer M., Loppin B., Heyer V., Degrave A., Woehl R., Lux A., Steffan T., Charbonnier X.Q. and Thisse C. (2001) Expression of the zebrafish genome during embryogenesis (NIH R01 RR15402). ZFIN Direct Data Submission.

(http://zfin.org)

Tian Z.J., An W. (2004) ERK1/2 contributes negative regulation to STAT3 activity in HSS-transfected HepG2 cells. Cell Res. Apr;14(2):141-7.

Wang J., Zhou M., Jin X., Li B., Wang C., Zhang Q., Liao M., Hu X., Yang M. (2019) Glycochenodeoxycholate induces cell survival and chemoresistance via phosphorylation of STAT3 at Ser727 site in HCC. J Cell Physiol. 2019;1–12.

Wegrzyn J., Potla R., Chwae Y.J., Sepuri N.B., Zhang Q., Koeck T., Derecka M., Szczepanek K., Szelag M., Gornicka A., Moh A., Moghaddas S., Chen Q., Bobbili S., Cichy J., Dulak J., Baker D.P., Wolfman A., Stuehr D., Hassan M.O., Fu X.Y., Avadhani N., Drake J.I., Fawcett P., Lesnefsky E.J., Larner A.C. (2009). Function of mitochondrial Stat3 in cellular respiration. *Science.* **323**(5915):793-7.

Wei W., Tweardy D.J., Zhang M., Zhang X., Landua J., Petrovic I., Bu W., Roarty K., Hilsenbeck S.G., Rosen J.M. and Lewis M.T. (2014). STAT3 signaling is activated preferentially in tumor-initiating cells in claudin-low models of human breast cancer. *Stem Cells*. **32**: 2571–2582.

SUPPLEMENTARY FIGURES
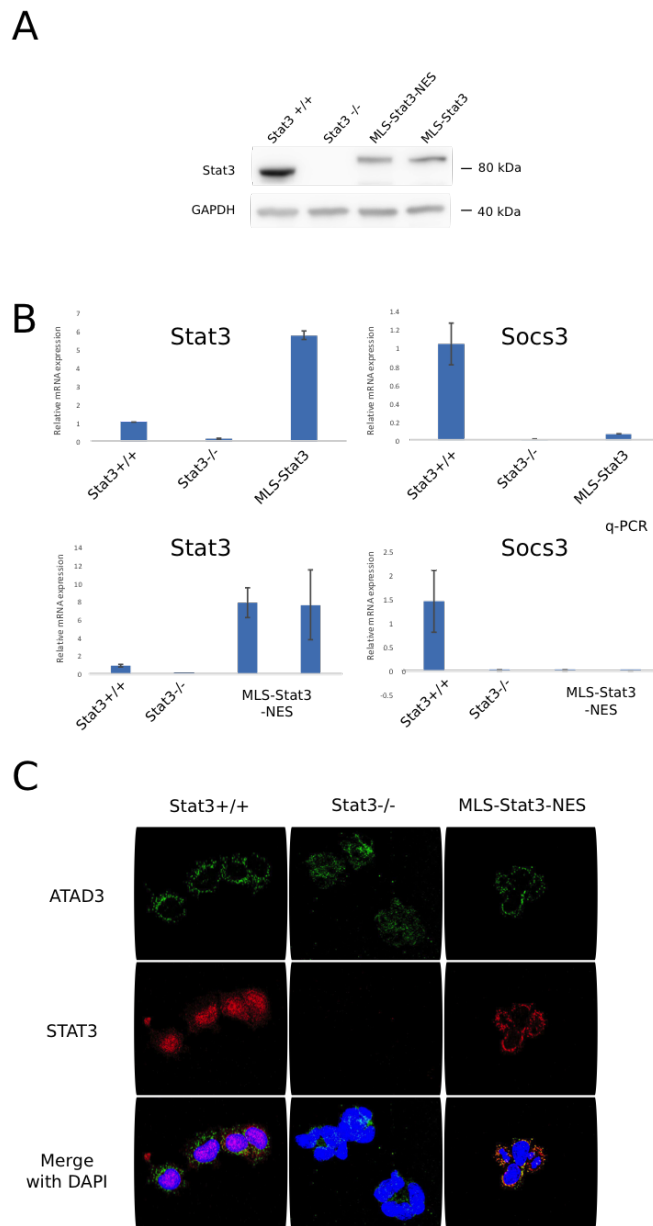
Fig. S1 **Validation of the *MLS_Stat3_NES* construct in murine Embryonic Stem Cells.** A: Western Blot for total STAT3 on wild-type (*Stat3*^{+/+}) or *Stat3* null cells (*Stat3*^{-/-}), or *Stat3* null cells transfected with the indicated constructs. Note the shift in molecular weight due to the presence of the MLS and NES tags. GAPDH serves as loading control. MLS = Mitochondrial Localization Signal. NES = Nuclear Export Sequence. B: qRT-PCR analyses of *Stat3*^{+/+}, *Stat3*^{-/-} and *Stat3*^{-/-} transfected with the *MLS_Stat3* (top panels) and *MLS_Stat3_NES* construct (bottom panels). *Stat3* mRNA levels are found increased upon transfection of both constructs (left), but the nuclear *Stat3* targets *Socs3* is mildly induced only by *MLS_Stat3*, but not by *MLS_Stat3_NES*. *ActinB* served as loading control and the expression is relative to *Stat3*^{+/+} cells. Two independent transfections for the *MLS_Stat3_NES* are shown as separate bars. C: Immunofluorescence staining for the mitochondrial marker ATAD3 and for STAT3 shows both nuclear and mitochondrial localization of endogenous STAT3 in wild-type cells, while in *Stat3*^{-/-} cells transfected with *MLS_Stat3_NES* we observed only mitochondrial localization.
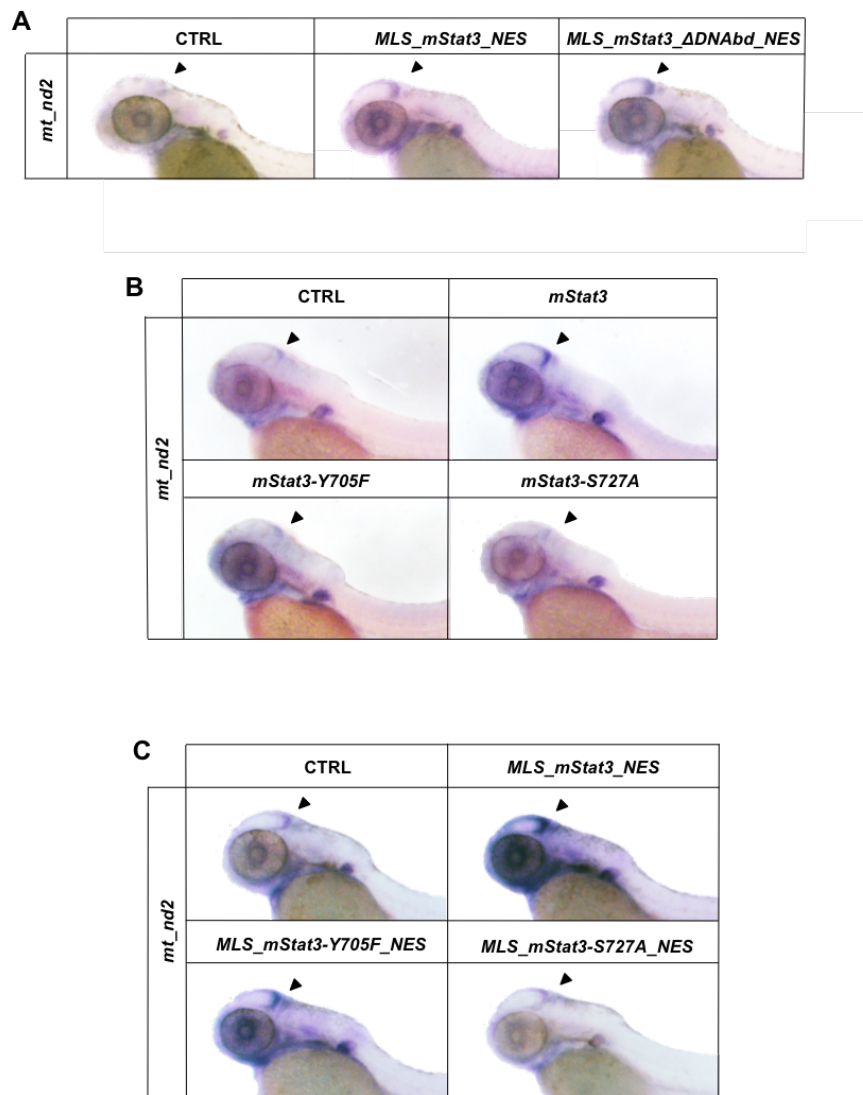
Fig. S2 **STAT3-dependent mitochondrial transcription depends on Y705 and S727 phosphorylations but not on STAT3 DNA binding domain.** A: WISH with anti-*mt_nd2* mRNA probe in 48-hpf uninjected embryos and embryos injected with indicated forms of mitochondria-targeted *mStat3* mRNA. B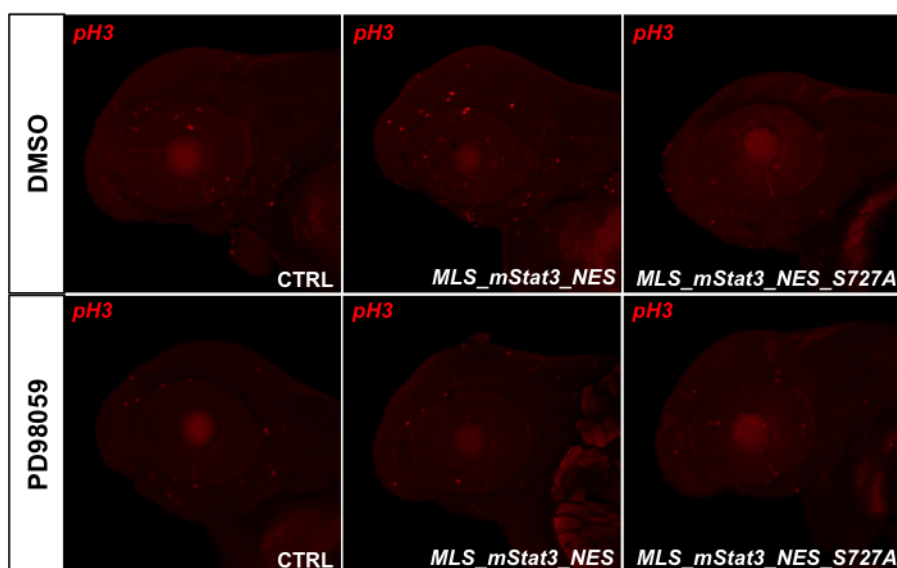: WISH with anti-*mt_nd2* mRNA probe in 48-hpf uninjected embryos and embryos injected with indicated forms of *mStat3* mRNA. C: WISH with anti-*mt_nd2* mRNA probe in 48-hpf uninjected embryos and embryos injected with indicated forms of mitochondria-targeted *mStat3* mRNA.

A

Fig. S3 **MEK-ERK pathway regulates mitoStat3-driven cell proliferation by phosphorylating STAT3 on S727 residue.** A: phospho-Histone-H3 (pH3) IF of WT embryos after treatment with DMSO or 12.5µM PD98059 from 24-48 hpf; zoom on the head.
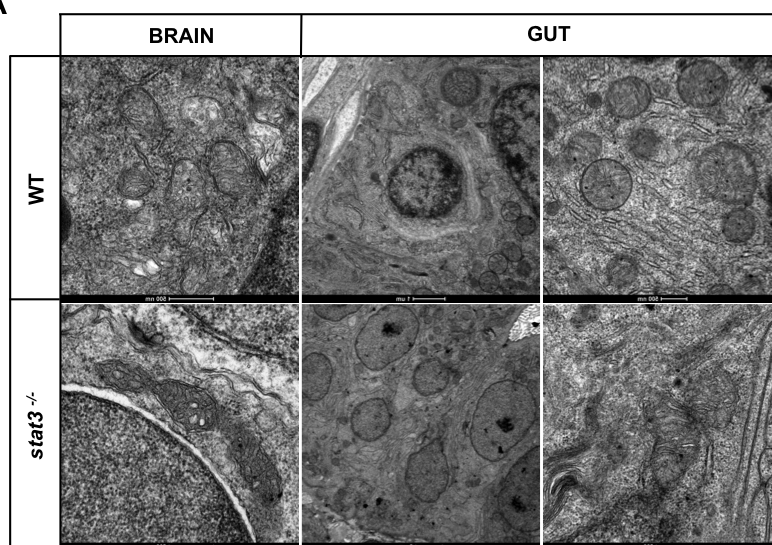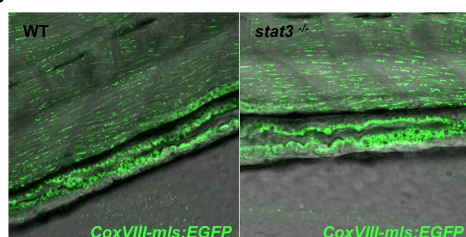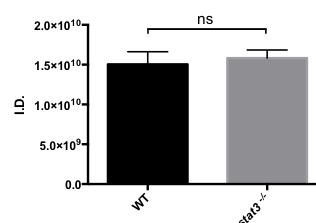

Fig. S4 **Stat3 depletion does not affect mitochondria morphology and biogenesis in the brain and intestine of stat3-/- larvae.** A: TEM analysis of mitochondrial morphology in intestine and brain of 6-dpf stat3-/- mutants and WT siblings. B: EGFP expression in the

intestine of 6-dpf *stat3−/−/Tg(CoxVIII-mls:EGFP)* and WT/*Tg(CoxVIII-mls:EGFP)* siblings (n=6). C: Fluorescence quantification of EGFP expression in the intestine of 6-dpf *stat3−/− /Tg(CoxVIII-mls:EGFP)* and WT/*Tg(CoxVIII-mls:EGFP)* siblings (p-value= 0,6878). Statistical analysis was performed by unpaired t-test on indicated number of samples*;* ns:not significant; error bars=SEM.
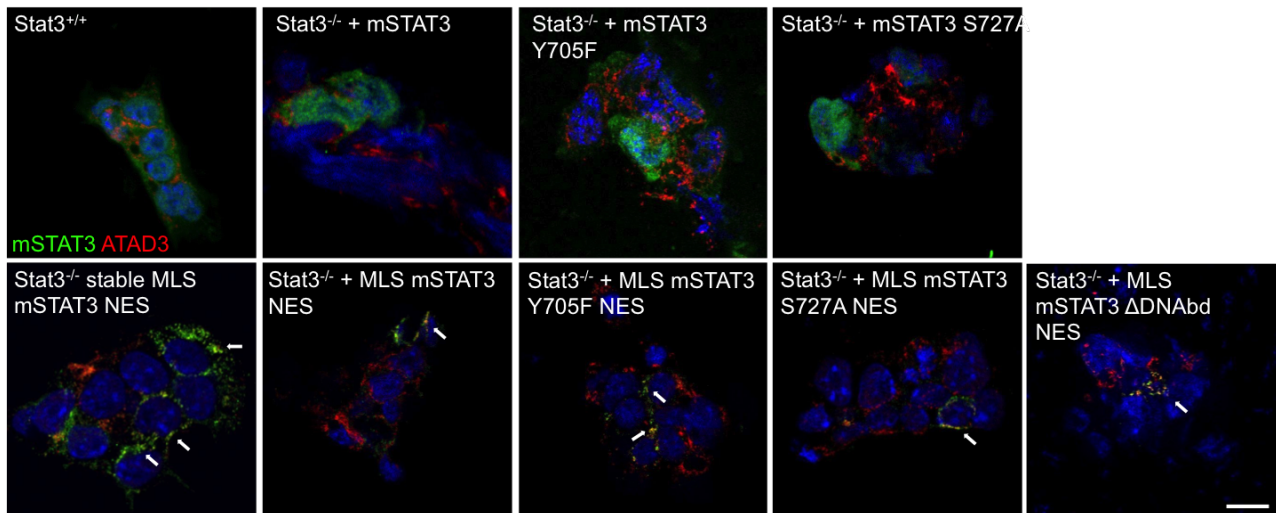
Fig. S5 **All mSTAT3 mutated forms targeted to the mitochondria localize within nucleoids near the mtDNA.** IF on mouse ES Stat3−/− cells transfected with the same plasmids used for the *in vitro* synthesis of the mRNA used in this study. Expression driven by a CMV promoter. The antibody reveals the effective overexpression and accumulation of cytosolic mSTAT3 (green) in all the isoforms shown in the top row. All the mito-targeted STAT3 perfectly colocalize with ATAD3 (in red) in the row below, a marker of mitochondrial nucleoids (white arrows). Scale bar = 10um. These pictures are the same used in Fig 2, 5 and 6 of the main text.

35
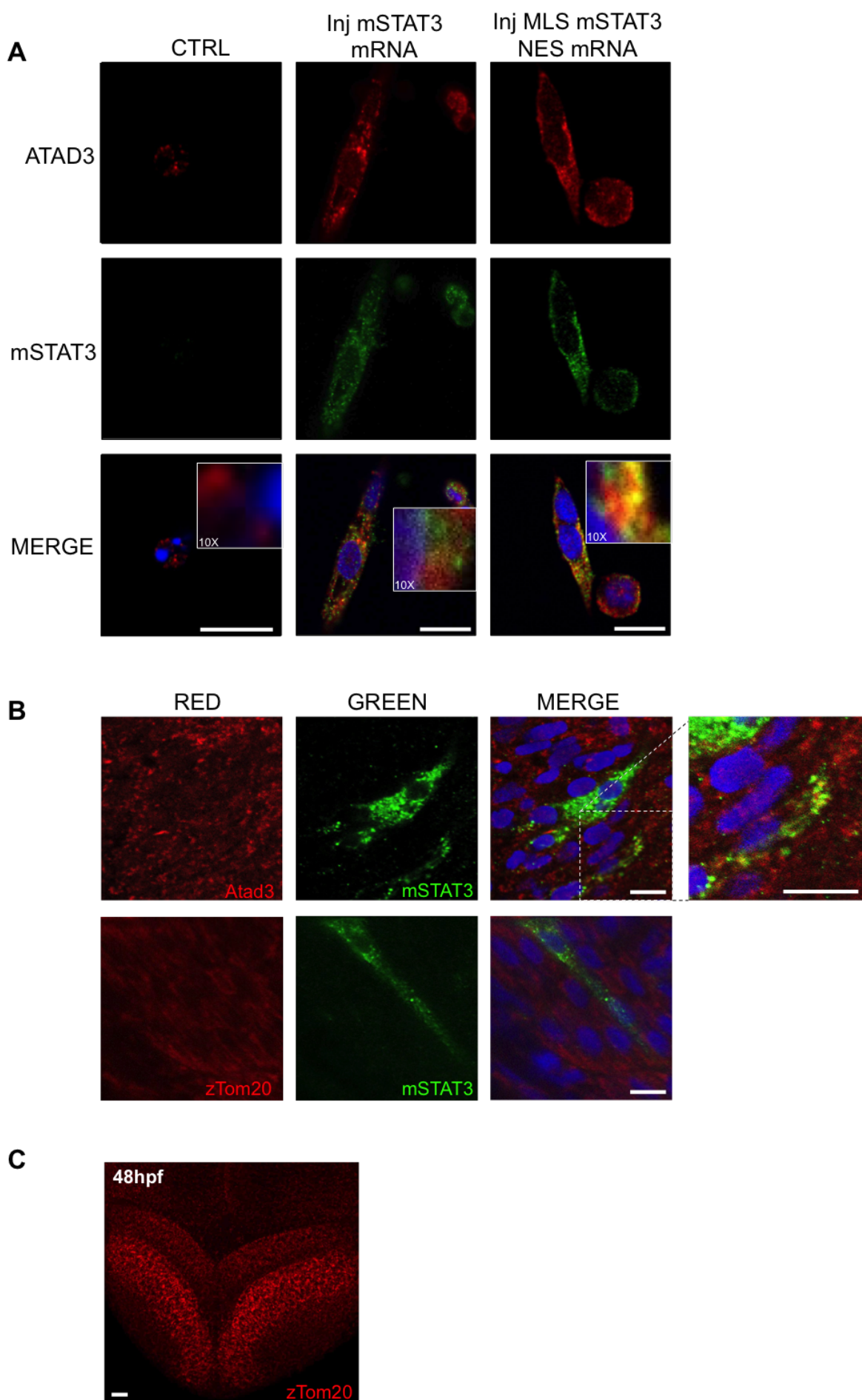
Fig S6 **Validation of the injected mRNAs on zebrafish.** A: IF on zebrafish cells, dissociated and plated from 24-hpf embryos injected with *mStat3* and *MLSmStat3* mRNA. The antibody reveals the expression of mSTAT3 (green). The mito-targeted STAT3 colocalize with ATAD3 (red), marker of mitochondrial nucleoids, confirming the correct subcellular localization of the protein. Conversely the analysis of mStat3 mRNA injected cells results in a delocalized staining inside the cells for mStat3 protein. Scale bar = 10um. B: Whole mount IF on 24-hpf zebrafish embryos injected with pCS2+MLS_mSTAT3_NES plasmid. The mosaic expression is driven by a CMV promoter to verify the intracellular localization of the murine protein. mSTAT3 (green) staining confirm the expected mitochondrial localization of the protein. The green pattern resembles the mitochondria shape and distribution, revealed in red by ATAD3 (in the upper panel) and TOM20 (in the panel below). Scale bar = 10um. C: IF anti Tom20 in the OT zone. The staining show that OT is the brain densest zone in mitochondria membranes in a 48-hpf zebrafish embryo.
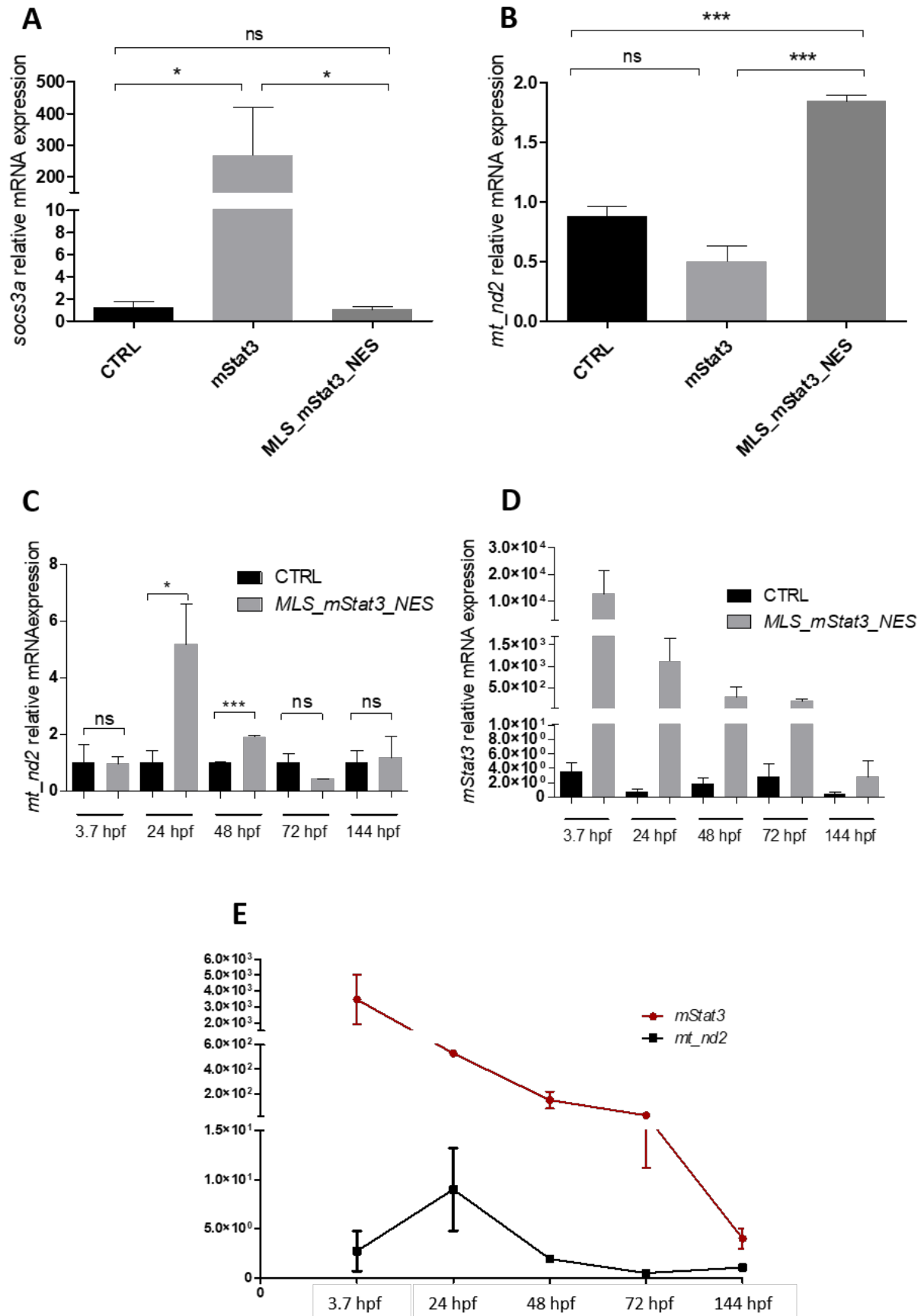
Fig S7 **Validation of effects of *mStat3* and *MLS_Stat3_NES* mRNA injected in zebrafish embryos** A: qRT-PCR analysis of *socs3a* mRNA levels in *mStat3* and *MLS_mStat3_NES* 48-hpf injected embryos. B: qRT-PCR analysis of *mt_nd2* mRNA levels in *mStat3* and

MLS_mStat3_NES 48-hpf injected embryos. C: qRT-PCR analysis of *mt_nd2* mRNA levels in injected larvae from 3.7 hpf to 6 dpf. D: qRT-PCR analysis of *mStat3* mRNA levels in injected larvae from 3.7 hpf to 6 dpf. E: Comparison between *mt_nd2* and *mStat3* transcript levels in injected larvae from 3.7 hpf to 6 dpf.